DMD Fast Forward. Published on May 30, 2019 as DOI: 10.1124/dmd.119.087718
This article has not been copyedited and formatted. The final version may differ from this version.

Defining the contribution of CYP1A1 and CYP1A2 to drug metabolism using humanized CYP1A1/1A2 and Cyp1a1/Cyp1a2 KO mice

Kapelyukh, Y., Henderson, C.J., Scheer, N., Rode, A. and Wolf, C.R.

Systems Medicine, School of Medicine, University of Dundee, Jacqui Wood Cancer Centre, Ninewells Hospital, Dundee, DD1 9SY, UK (YK, CJH, CRW).

Taconic Biosciences Inc., Rensselaer, NY 12144 (NS, AR)

Current affiliation - FH Aachen, University of Applied Sciences, Heinrich-Mußmann-Str.1, 52428 Jülich, Germany (NS); F. Hoffmann-La Roche, Grenzacherstrasse 1244070 Basel, Switzerland (AR)

DMD # 87718

Running Title: hCYP1A1/1A2 mice for drug interaction studies

Corresponding Author

Professor C. Roland Wolf, School of Medicine, University of Dundee, Jacqui Wood Cancer Centre, Ninewells Hospital, Dundee, DD1 9SY, UK.

c.r.wolf@dundee.ac.uk

01382-383133

Text pages 25

Tables 3

Figures 11

References 66

Words in Abstract 191

Words in Introduction 748

Words in Discussion 1566

Non-standard abbreviations:

CAR – Constitutive androstane receptor; ER – 7-ethoxyresorufin; EROD 7-ethoxyresorufin O-deethylation; HLM – human liver microsomes; HRN – Hepatic Reductase Null mice; MR- 7-methoxyresorufin; MROD - 7-methoxyresorufin O-demethylation; PBPK – physiologically based pharmacokinetics; TCDD - 2, 3, 7, 8-tetrachlorodibenzodioxin; PXR – Pregnane X receptor;

Abstract

Cytochrome P450s, CYP1A1 and CYP1A2 can metabolize a broad range of foreign compounds and drugs. However, these enzymes have significantly overlapping substrate specificities. In order to establish their relative contribution to drug metabolism *in vivo* we have used a combination of mice humanized for CYP1A1 and CYP1A2 together with mice nulled at the Cyp1a1 and Cyp1a2 gene loci. CYP1A2 was constitutively expressed in the liver and both proteins were highly inducible by TCDD in a number of tissues including liver, lung, kidney and small intestine. Using the differential inhibition of the human enzymes by quinidine we have developed a method to distinguish the relative contribution of CYP1A1 or CYP1A2 in the metabolism of drugs and foreign compounds. Both enzymes made a significant contribution to the hepatic metabolism of the probe compounds 7-methoxy and 7-ehthoxyresorufin in microsomal fractions from animals treated with TCDD. This enzyme kinetic approach allows modelling of the CYP1A1, CYP1A2 and non-CYP1A contribution to the metabolism of any substrate, at any substrate, inhibitor or enzyme concentration and as a consequence can be integrated to a PBPK model. The validity of the model can then be tested in the humanised mice *in vivo.*

Significance Statement:

Human CYP1A1 and CYP1A2 are important in defining the efficacy and toxicity/carcinogenicity of drugs and foreign compounds. In the light of differences in substrate specificity and sensitivity to inhibitors, it is of central importance to understand their relative role in foreign compound metabolism. To address this issue, we have generated mice humanized or nulled at the Cyp1a gene locus and through the use of these mouse lines and selective inhibitors, developed an enzyme kinetic-based model to enable more accurate prediction of the fate of new chemicals in man, and which can be validated *in vivo* using mice humanised for cytochrome P450-mediated metabolism.

Introduction

CYP1A2 is a major cytochrome P450 which accounts for ~12% of the total hepatic P450 content in humans (Iwatsubo et al., 1997; Achour et al., 2014). CYP1A2 substrates include drugs, industrial chemicals and environmental toxicants. The enzyme activity is variable in man due to a combination of genetic polymorphism and environmental factors affecting enzyme expression level and activity. The expression of both CYP1A1 and CYP1A2 are highly regulated by the aryl hydrocarbon receptor (AHR). In the case of hepatic CYP1A2 this can be induced up to 10-fold by AHR ligands (Abraham et al., 2002). The activated AHR binds to xenobiotic response elements on the 5' flanking region of CYP1A2 gene. As this element is shared between *CYP1A2* and *CYP1A1* genes, many *AHR* and even some CAR ligands simultaneously induce both enzymes (Corchero et al., 2001; Ueda et al., 2006; Yoshinari et al., 2008; Yoshinari et al., 2010). The active sites of both CYP1A1 and CYP1A2 have a CYP1 family-specific distortion of the F helix in the area of the substrate binding cavity, causing bending of the helix and resulting in the formation of an enclosed and planar substrate binding site. This explains the overlapping substrate and inhibitor specificities for both enzymes (Sansen et al., 2007; Walsh et al., 2013).

For example, CYP1A1 and CYP1A2 both activate many pro-carcinogens and/or participate in their detoxification (Nebert et al., 2013; Stiborova et al., 2014). In certain cases they also mediate the elimination/metabolic activation of drugs (Lin et al., 2017). As a consequence, for any studied AHR ligand (potential environmental toxicant or new pharmaceutical chemical entity) the individual contribution of both CYP1A1 and CYP1A2 to compound elimination in man needs to estimated using physiologically based pharmacokinetic (PBPK) models (Andersen et al., 1997; Santostefano et al., 1998; Cortessis and Thomas, 2004). Particular attention has to be given to AHR-mediated induction of the enzymes, as this can markedly affect the relative contribution of CYP1A1 and CYP1A2 to metabolism. For example, 7-ethoxyresorufin O-deethylation (EROD) in untreated rat liver microsomes is catalysed by CYP2C6, CYP2B1, CYP2C11 and CYP3A1/2, whilst the same compound is oxidised

predominantly by CYP1A1 in microsomes from 3-methylcholantrene treated rats with CYP1A2 playing a secondary role (Burke et al., 1994). Similarly, whilst CYP1A2 is considered the sole enzyme catalysing 7-methoxyresorufin O-demethylation (MROD) in liver microsomes from untreated rats (Burke et al., 1994; Floreani et al., 2012), experimental data suggest CYP1A1 to be a second major enzyme involved in the reaction in the liver microsomes from safrole (Burke et al., 1994) or benzo[a]pyrene treated animals (Floreani et al., 2012).

Recombinant rat CYP1A1 is ~59 times more active in EROD, and ~14 times less active in MROD, than CYP1A2 (Namkung et al., 1988) suggesting that 7-ethoxyresorufin (ER) and 7-methoxyresorufin (MR) are selective substrates for the rat CYP1A1 and CYP1A2 respectively. However, recombinant human CYP1A1 is only ~2.8 times more active in EROD and ~5.8 times less active in MROD compared to human CYP1A2 indicating more extensive overlap in substrate specificity (Liu et al., 2004). The accuracy of estimates of toxicological risk or drug pharmacokinetic data generated in rodents to man is often compromised by the species differences in metabolism (Cheung and Gonzalez, 2008) and in a number of cases differences between rodent and human CYP1A1 and CYP1A2 (Turesky et al., 1998; Turteltaub et al., 1999; Shinkyo et al., 2003). One approach to improve the predictive power of animal models involves humanisation for the relevant xenobiotic metabolising enzyme (Cheung and Gonzalez, 2008). Mouse models humanised for CYP1A1 and/or CYP1A2 have demonstrated human-like pro-carcinogen activation/detoxification patterns for 2-amino-1-methyl-6-phenyl-imidazola[4,5-b]pyridine (Cheung et al., 2005) and aristolochic acid I (Levova et al., 2012).

In this study two new mouse models are described. In one (hCYP1A1/1A2) both mouse *Cyp1a1* and *Cyp1a2* were replaced with the corresponding human orthologues. The second model (Cyp1a KO) is a *Cyp1a1* and *Cyp1a2* knock-out. The expression of the Cyp1a/CYP1A enzymes was measured in liver and extrahepatic tissues of vehicle and 2,3,7,8-tetrachlorodibenzo-p-dioxin (TCDD)-treated animals. A method for the assessment of relative contribution of CYP1A1 and CYP1A2 to EROD and MROD was developed using the CYP1A1 selective inhibitor quinidine. The method was applied to measure individual contributions of

human CYP1A1 and CYP1A2 to EROD and MROD in liver microsomes from TCDD-treated humanised mice. Values of fraction metabolised by CYP1A2 were determined for the CYP1A2 substrates tacrine, ramelteon and caffeine in untreated humanised and wild-type (WT) animals. The utility of this mouse line relative to the recently created more complex P450 humanised model (Henderson et al., 2019) is discussed.

Materials and Methods

Generation of hCYP1A1/1A2 and Cyp1a KO mice.

hCYP1A1/1A2 and Cyp1a KO mice were generated in a collaboration between CXR Biosciences (now Concept Life Sciences) and Taconic Biosciences in a project funded by the Scottish Government through the ITI programme (principal investigators CRW and NS) as detailed below. Culture and targeted mutagenesis of embryonic stem (ES cells) were carried out as described previously (Behringer et al., 2014). The murine *Cyp1a1 and Cyp1a2* gene loci were successively modified by homologous recombination in C57BL/6NTac mouse ES cells with two targeting vectors, such that the genomic sequences between the translational start ATGs and the stop codons of mouse *Cyp1a1* and *Cyp1a2* were replaced with the orthologous genomic sequences of human *CYP1A1* and *CYP1A2*, respectively (**Supplemental Figure 1**) and therefore removing the murine Cyp1a1 and Cyp1a2 genes. Southern blot analysis was used to identify correct double targeted clones, which were injected into BALB/c-blastocysts and transferred into foster mothers as described previously (Behringer et al., 2014). Chimeric mice were bred to a germline flipase (Flpe) deleter strain to remove selectable markers (**Supplemental Figure 1**) as described previously (Scheer et al., 2012a). Heterozygous *CYP1A1/1A2* humanized mice were identified by PCR and either crossed with each other to generate homozygous hCYP1A1/1A2 mice or crossed to a deleter strain expressing Cre-recombinase to remove the *Cyp1a* gene locus from the germ line (**Supplemental Figure 1**). Heterozygous *Cyp1a* knockout offspring were identified by PCR and further crossed to generate homozygous Cyp1a KO mice. The Flpe- and Cre-deleter strains mentioned above were generated in-house on a C57BL/6NTac genetic background.

Animal accommodation and husbandry

Animal procedures were performed under licence from the UK Home Office (Animal (Scientific Procedures) Act (1986), and 2010/63/EU) and after approval by the Ethical Review Committee, University of Dundee. Homozygous mice for each transgenic line were used for experimental studies. C57BL/6NTac mice were used as WT controls. Mice were kept in open-

top cages with *ad libitum* access to food (RM1; Special Diet Services Ltd., Essex, UK) and drinking water, and acclimatized for at least 5 days before study commencement. Room temperature was between 19 - 23°C and relative humidity 40 - 70%, with a 12-h light/dark cycle (Scheer et al., 2012b).

TCDD treatment

Mice were given a single intra-peritoneal (i.p.) dose of TCDD (10 µg/kg) or vehicle control (corn oil) and then euthanized 48 hours after the dosing using a rising concentration of CO_2.

Tissue collection

Venous blood was removed by cardiac puncture and dispensed into lithium/heparin-coated tubes. Red blood cells were removed by centrifugation (16.1 krcf for 10min at room temperature) and the supernatant (plasma) was stored at approximately -70°C.

The gall bladder was removed, and then the liver was removed, weighed and scissor-minced in ice-cold KCl (1.15% w/v) for subsequent liver subcellular fractionation. The small intestine and colon were removed and flushed with ice cold phosphate-buffered saline (PBS) containing a protease inhibitor cocktail (Roche Diagnostics, Basel, Switzerland).

The duodenum, jejunum, ileum and colon sections (approximately 10 cm each) were transferred into separate tubes, flash frozen immediately in liquid nitrogen and stored at approximately –70^{o}C prior to the preparation of microsomes. The heart, lungs, brain, spleen, testis and kidneys were removed from each animal, flash frozen in liquid nitrogen and stored at approximately -70^{o}C prior to microsome preparation.

Preparation of microsomes

Microsomal fractions were prepared as previously described (Henderson et al., 2019). Briefly, fresh liver samples were homogenized in ice-cold SET buffer (0.25 M sucrose, 5 mM EDTA, 20 mM Tris-HCL, pH 7.4; 9 ml buffer/g liver) and centrifuged at 2000 rpm (Sorvall RTH-250,10

minutes, 4°C). The supernatant was centrifuged (12000 rpm, Sorvall SS-34 rotor, 20 minutes, 4°C) and the resulting supernatant centrifuged at (~30000rpm, Sorvall TFT-45.6, 90 minutes 4°C), and microsomal pellets resuspended in ice-cold SET buffer and stored at -70°C.

Frozen individual duodenum, ileum, jejunum and colon samples and pooled (one pool per experimental group) lung, kidney, spleen, heart, brain and testes were homogenized in SET buffer containing protease cocktail inhibitor (Roche) and PMSF (1 mM) using a Polytron homogenizer. Microsomal fractions were prepared as described above for liver tissue.

Biochemical Measurements

Clinical Chemistry

The activity of alanine aminotransferase and concentration of albumin in the plasma samples were measured in the Clinical Pathology Service Laboratory (Mary Lyon Centre, Harwell, UK).

Total Protein and P450 Determination

Microsomal protein concentration fractions was measured using a modification of a previously described method (Lowry et al., 1951) and total hepatic microsomal P450 as previously described (Omura and Sato, 1964).

Immunoblotting

The expression of Cyp1a, CYP1A1 and CYP1A2 in pooled liver, duodenum, ileum, jejunum, colon, lung, kidney, spleen, heart, brain and testis microsomal samples was determined by immunoblot analysis using primary antibodies against recombinant rat CYP1A2 (Forrester et al., 1992), human CYP1A1 and CYP1A2 (AB1258, Millipore, UK and PAP 021, Cypex/Nosan, UK respectively), loading 20 µg of microsomal protein per lane. The positive standards were membrane preparations from bacteria expressing recombinant human CYP1A1 (0.36 pmol) or CYP1A2 (1 pmol). Protein expression was visualised using Immobilon Western chemiluminescent detection (Millipore) according to manufacturer's instructions, and data

collected and processed (contrast/brightness adjusted identically for each across the entire image) using a FujiFilm LAS-3000 mini CCD system and the device software Version 2.2. Acquired images were saved in the Tagged Image File Format using software MultiGauge (Fuji Film) and transferred to Power Point using Picture Manager (Microsoft Office 2010).

7-Ethoxyresorufin O-deethylation and 7-methoxyresorufin O-demethylation

A mixture of ER (0.93 μM) or MR (0.46 μM) and liver microsomes (0.004-0.27 mg protein/ml) in 100 mM potassium phosphate buffer (pH 7.4) supplemented with $MgCl_2$ (3.3 mM) was incubated at 37°C for 5 min before the reaction was initiated by injection of NADPH (final concentration 1.2 mM). Generation of the fluorescent product was registered in a kinetic mode using Fluoroscan Ascent FL (Labsystems; excitation filter 530 nm; emission filter 584 nm). Slopes of the linear part of the kinetic curves were calculated using Ascent Software Version 2.4.1 (Labsystems). For each well with the reaction media there was a control well containing the reaction mixture with resorufin (4 pmol). Before addition of NADPH to the reaction wells, fluorescence was recorded both from the reaction and from the control wells. The average fluorescence was calculated and the difference between wells with and without resorufin was used for the conversion of the relative fluorescence units to the picomoles of the reaction product. Activities in duodenum, ileum, jejunum, colon, lung, kidney, spleen, heart, brain and testis microsomes were measured as described above except for the following adjustments: MR concentration was 1 μM, concentration of total microsomal protein in the reaction was in a range of 0.07-0.43 mg/ml and amount of resorufin added to calculate the reaction product concentration was 40 pmol.

Inhibition of recombinant CYP1A1 and CYP1A2 by quinidine

A mixture of MR (0.57 μM) and microsomes (3.46 pmol/ml CYP1A1 or 10.8 pmol/ml CYP1A2; 0.25 mg protein/ml adjusted using Control Bactosomes (Cypex, UK)) in phosphate buffer (100

mM KH_2PO_4 pH7.4, 3.3 mM $MgCl_2$) was incubated with quinidine (0-2 mM) in a microtiter plate reader for 5 min at 37°C prior to the start of the reaction by addition of NADPH (final concentrations 1.2 mM). Generation of fluorescent product was registered in a kinetic mode (excitation filter 530; emission filter 584 nm). Slopes of the linear part of the kinetic curves were calculated using Ascent Software Version 2.4.1 (Labsystems).

Estimation of individual contribution of CYP1A1 and CYP1A2 to EROD and MROD in liver microsomes from hCYP1A1/1A2 mice

A mixture of ER or MR (0.039-5 μM) and microsomes in phosphate buffer (100 mM KH_2PO_4 pH7.4, 3.3 mM $MgCl_2$) was incubated with quinidine (0, 30 and 200 μM (except for MROD catalysed by recombinant CYP1A1, where quinidine was at 0, 6 and 30 μM)) in a microtiter plate reader for 5 min at 37°C prior to the start of the reaction by addition of NADPH (final concentrations 1.2 mM). Protein enzyme/concentrations were 3.46 pmol/ml for recombinant human CYP1A1, 10.8 pmol/ml for recombinant human CYP1A2, 0.05 mg protein/ml for liver microsomes from TCDD treated hCYP1A1/1A2 mice, 0.25 mg protein/ml for liver microsomes from TCDD treated Cyp1 KO mice and vehicle treated hCYP1A1/1A2 mice. Where needed total protein concentration in the reaction mixtures was adjusted using Control Bactosomes (Cypex, UK), so all reactions (including those with the recombinant cytochromes P450) were carried out at a total protein concentration of 0.25 mg protein/ml. Generation of fluorescent product was registered in a kinetic mode (excitation filter 530; emission filter 584 nm). Slopes of the linear part of the kinetic curves were calculated using Ascent Software Version 2.4.1 (Labsystems). For each well with the reaction media there was a control well containing the reaction mixture with resorufin (40 pmol). Before addition of NADPH to the reaction wells, fluorescence was recorded both from the reaction and from the control wells. The average fluorescence was calculated and the difference between wells with and without resorufin was used for the conversion of the relative fluorescence units to the picomoles of the reaction product. The selected quinidine concentrations provided marked CYP1A1 inhibition which is

essential for precise calculation of inhibition constants (Kakkar et al., 2000) whilst leaving sufficient enzyme activity for accurate measurement. Kinetic parameters of quinidine inhibition of rCYP1A1 are presented in **Table 1**.

Microsomal stability of ramelteon and tacrine

A 880 μl mixture of ramelteon (1.25 μM) and C57BL6J (WT), Cyp1a KO, hCYP1A1/1A2 or pooled human liver microsomes (0.625 mg protein/ml) in phosphate buffer (100 mM KH_2PO_4 pH7.4, 3.3 mM $MgCl_2$) was incubated for 5 min at 37°C in a water bath before an 80 μl aliquot was mixed with 100 μl of ice-cold methanol containing tacrine (100 ng/ml) as an internal standard, followed by addition of 20 μl of NADPH solution (6 mM) in the phosphate buffer. The reaction was started by addition of 200 μl NADPH to the remaining mixture of ramelteon with microsomes and 100 μl aliquots were taken at 1, 2, 5, 10, 15, 20 and 30 min after the reaction start, mixed with equal volume of ice-cold methanol containing the internal standard, incubated on ice for at least 20 min and centrifuged for 15 min at 16,000 rcf and +4°C on Centrifuge 5415 R (Eppendorf, Hamburg, Germany). Control incubations were carried out without the cofactor or microsomes. The concentration of ramelteon in the supernatant was measured by HPLC-MS/MS. Chromatographic separation was performed on a Prodigy Phenyl-3 column (5 μm, 50 x 2.0 mm) (Phenomenex) using an injection volume of 10 μl and a run time of 7 minutes. Mobile phase consisted of 0.1% solutions of formic acid in water (solvent A) and acetonitrile (solvent B). For elution a linear gradient from 20% to 60% of solvent B in 4 min was used, following by 3 min equilibration at 20% B. The multiple reaction monitoring parameters for ramelteon and tacrine were 260.28, 199.2 (precursor ion) and 204.21, 171.11 (product ion) respectively. The concentrations of ramelteon were calculated from the calibration curve. Tacrine microsomal stability was measured as described for ramelteon except for the final microsomal protein concentration was 1 mg/ml, the reaction aliquots were collected at 5, 10, 20, 30, 40 50 and 60 min after the reaction start and the reaction was

stopped by mixing with 120 μl of 167 mM hydrochloric acid containing 183 ng/ml caffeine as internal standard. The mobile phase gradient started at 5% B. The multiple reaction monitoring parameters for tacrine and caffeine were 199.2, 195.18 (precursor ion) and 171.11, 138.07 (product ion) respectively.

Caffeine pharmacokinetics

Caffeine (5 mg/kg; 10ml/kg; dissolved in 50 mM sodium citrate buffer (pH4.7)) was delivered to WT, Cyp1a KO and hCYP1A1/1A2 mice (4 animals per experimental group) by oral administration. A separate experimental group consisted of mice with conditionally deleted hepatic P450 oxidoreductase (Henderson et al., 2003) (Hepatic Reductase Null (HRN) mice) Whole blood samples from WT and hCYP1A1/1A2 mice were collected at 12 min; 24 min; 40 min; 1h; 2h; 3h; 4h; 6h and 8h after the administration. Whole blood samples from HRN and Cyp1a1/1a2 KO mice were collected at 12 min; 24 min; 40 min; 1h; 3h; 6h, 8h, 12h and 24h post-administration. The collected whole blood samples (10 μl) were mixed with equal volume of heparin solution in water (15 U/ml), frozen in liquid nitrogen and stored at -70°C. The concentration of caffeine in whole blood was measured by LC-MS/MS. Calibration standards were prepared by spiking whole mouse blood with an appropriate amount of caffeine standard and mixing the whole blood aliquots with an equal volume of heparin solution in water (15 U/ml). The test samples and calibration standards (20 μl) were mixed with 80 μl of perchloric acid (1.5%) containing tacrine (50 ng/ml) as internal standard, vortexed and centrifuged at 16,100 rcf for 15 minutes. The supernatant was collected, and the centrifugation step was repeated. The supernatant was transferred to a 96-well plate and caffeine concentration measured by HPLC-MS/MS from the calibration curve using the same conditions as those described for tacrine.

Pharmacokinetic parameters were calculated using Phoenix WinNonlin version 6.4 (Certara, St. Louis, USA).

Full details of data analysis are given in **Supplemental Data**.

Results

Generation of hCYP1A1/1A2 and Cyp1a KO mice

Homozygous hCYP1A1/1A2 and Cyp1a KO mice appeared normal, could not be distinguished from WT animals and had normal survival rates. There were only minor differences between the different lines with or without TCDD treatment as shown in **Supplemental Table 1**.

Total cytochrome P450

Total hepatic cytochrome P450 content in untreated WT, hCYP1A1/1A2 and Cyp1a KO mice was similar suggesting that Cyp1a1 and Cyp1a2 are only minor constitutive P450 forms (**Figure 1**). Administration of TCDD resulted in a significant increase of total hepatic cytochrome P450 in WT mice (2.37-fold, from 355 to 840 pmol/mg protein) and hCYP1A1/1A2 (1.84-fold, from 344 to 632 pmol/mg protein). As there was no change in total P450 in Cyp1a KO on TCDD treatment the increase was attributable to the induction of CYP1A enzymes in WT and hCYP1A1/1A2 mice, which accounted for 58 and 46% of the total hepatic P450 content, respectively**.**

CYP1A1 and CYP1A2 protein expression and activity

Western blot analysis showed that CYP1A1 was not expressed constitutively in the humanised mouse liver but CYP1A2 was (**Figure 2A, B**). Neither protein was expressed constitutively in any other tissue. Bands observed in vehicle control samples on **Figure 2A** and also visible in Cyp1a KO microsomes on **Figure 2D** are likely due to non-specific binding of CYP1A1 antibodies. On TCDD treatment both CYP1A1 and CYP1A2 were induced in the liver, and in the case of CYP1A1 also in the lung and duodenum with a low level of induction in the ileum and jejunum. The induction appeared to be less than that for Cyp1a1 in WT animals (**Figure 2C**) but this may relate to the antibodies used. As expected, both Cyp1a1 and Cyp1a2 (*data not shown*) could not be detected in the KO animals irrespective of TCDD treatment.

EROD activity in liver microsomes from Cyp1a KO mice was decreased by 22% relative to WT animals whilst the constitutive activity was slightly increased (to 155%) in hCYP1A1/1A2 mice (**Figure 3A**). Treatment with TCDD resulted in a marked (~114-fold) increase in EROD activity in WT and 39-fold in hCYP1A1/1A2 mice relative to untreated animals**.** A 3-fold increase in Cyp1a KO liver was also observed. MROD was decreased by approximately 90% in liver microsomes from Cyp1a KO mice compared to WT animals, whilst in the hCYP1A1/1A2 mouse line the activity was unchanged (**Figure 3B**). On TCDD treatment of WT and hCYP1A1/1A2 mice 44- and 31-fold increases in MROD activities were measured, respectively. A small increase in activity (4.6-fold) was also measured in the Cyp1a KO line.

Both EROD and MROD activities were below the limit of detection in all extrahepatic tissues in all the mouse models. On TCDD treatment these activities were induced in several tissues of both WT and hCYP1A1/1A2 mice. The highest activity for both substrates was in the lungs with significant activity in the duodenum and other regions of the gastrointestinal tract. These data are consistent with the Western blot analysis of CYP1A1 expression (**Figure 3A, C**). Interestingly, the humanised samples exhibited higher activities than WT samples for these substrates.

Estimation of the relative contribution of CYP1A2 to EROD and MROD activities

Quinidine is a known inhibitor of the human P450 enzymes CYP2D6 and CYP1A1 but not CYP1A2 (Ching et al., 2001). As CYP2D6 is not involved to any significant extent in either EROD (McGinnity et al., 1999) or MROD (Burke et al., 1994), quinidine was used as CYP1A1 specific inhibitor in this study. Consistent with the literature (Ching et al., 2001), recombinant CYP1A1-mediated MROD was strongly inhibited by quinidine (**Figure 4**), IC50=5.8 μM) with CYP1A2 having a much lower affinity (1977 μM). We used this difference to determine the relative contribution of CYP1A1, CYP1A2 and cytochromes P450 other than CYP1A to ER and MR metabolism in liver microsomes from TCDD-treated hCYP1A1/1A2 mice. The overall rate of EROD or MROD was assumed to be the addition of rates from the CYP1A1, CYP1A2

and non-Cyp1a components. Initially, the interaction of substrate and quinidine with each one of the above components was studied individually using human recombinant CYP1A1, CYP1A2 and microsomes from TCDD-treated Cyp1a KO mice. For human CYP1A1, EROD and MROD inhibition by quinidine was consistent with a mixed and competitive mechanism respectively **(Table 1; Supplemental Scheme 1a, d; Figure 5A, B; Eq. 1; Eq. 4).** Quinidine did not inhibit either EROD or MROD activity catalysed by CYP1A2 **(Table 1; Supplemental Scheme 1b, e; Figure 5C, D; Eq. 2; Eq. 5).** In TCDD-treated Cyp1a KO samples both EROD and MROD were inhibited non-competitively with high K_i values (>200 μM) **(Table 1; Supplemental Scheme 1c, f; Figure 5E, f; Eq. 3; Eq. 6).** Substrate and quinidine binding constants were calculated for all of the reactions measured above (**Table 1**) and used in **Eq. 7** and **Eq. 8**, to relate EROD and MROD reaction rates to concentrations of substrate and quinidine. It was assumed that the substrate and quinidine binding affinities of recombinant CYP1A1 and CYP1A2 are the same as those of CYP1A1 and CYP1A2 in liver microsomes from TCDD-treated hCYP1A1/1A2 mice. Also, that the non-Cyp1a component of both EROD and MROD in hCYP1A1/1A2 mice corresponds to the total EROD and MROD in Cyp1a KO mice. V_{max} values for EROD and MROD of the non-Cyp1a component were those calculated from experiments using liver microsomes from TCDD-treated Cyp1a KO mice. As a result, **Eq. 7** and **Eq. 8** are left with two independent variables, namely substrate and quinidine concentrations, and two parameters (V_{max} for CYP1A1 and CYP1A2). These V_{max} values were calculated by non-linear regression analysis of reaction rates in microsomes from TCDD-treated hCYP1A1/1A2 mice at different concentrations of quinidine and ER (**Figure 6A**) or MR (**Figure 6B**) using **Eq. 7** and **Eq. 8**, respectively. The V_{max} values for CYP1A1 and CYP1A2 were 2800 and 1900 pmol/min/mg protein for EROD, and 1600 and 2000 pmol/min/mg protein for MROD, respectively.

With these V_{max} values, all parameters in **Eq. 7** and **Eq. 8** became known, which allowed simulation of the reaction rates in liver microsomes from hCYP1A1/1A2 mice for any given substrate and quinidine concentration, not only for the general reaction but also for the

individual CYP1A1, CYP1A2 and non-Cyp1a contributions. Using these equations, the contribution of each individual enzymatic component in liver microsomes from TCDD-treated hCYP1A1/1A2 mice for EROD (**Figure 6E**; **Eq. 9-11**) and MROD (**Figure 6D, F**; **Eq. 12-14**) was calculated. In the absence of quinidine, the CYP1A1 contribution to EROD at low (10pM) substrate concentration was calculated to be ~94% (**Figure 6C**). This decreased to 70% at 1μM ER and further reduced to ~51% at 6μM substrate. Correspondingly, the contribution of CYP1A2 was increased from ~4.8% at low substrate concentration to ~45% at 6μM ER. The non-Cyp1a contribution was in a range from 0.8 to 3.9 %. At a quinidine concentration of 200μM and low concentration of ER the CYP1A1, CYP1A2 and non-CYP1A contributions were ~22%, 70% and 8% respectively and did not change substantially with rise of ER concentration.

CYP1A1 and CYP1A2 contributions to MROD activity were almost equal (49% and 50% respectively) at low substrate concentrations in the absence of inhibitor (**Figure 6D**). As MR concentration increased the CYP1A1 contribution decreased and CYP1A2 contribution increased, at 6μM MR being ~18% and ~81% respectively. At low concentrations of MR and 200μM quinidine the reaction was almost exclusively catalysed by CYP1A2 (~98% contribution) with CYP1A1 impact being less than 1% (**Figure 6F**). As the substrate concentration increased CYP1A2 contribution decreased to ~90% and CYP1A1 increased to ~9%. Non-Cyp1a contribution to MROD did not exceed 1.5%. In liver microsomes from vehicle-treated hCYP1A1/1A2 mice 200 μM quinidine resulted minor inhibition of the EROD which was highest (~20 %) at high substrate concentrations (**Figure 7A**). MROD was not affected by the inhibitor (**Figure 7B**).

Human recombinant CYP1A1 and CYP1A2 reconstituted from purified enzymes have been reported to have an EROD/MROD activity ratio of 6.5 and 0.4, respectively at 10μM substrate (Liu et al., 2004). The EROD/MROD ratio for CYP1A1 in hCYP1A1/1A2 liver microsomes was calculated by **Eq. 1** and **Eq. 4** using the following assumptions: 1) 10μM substrate

concentration; 2) absence of inhibitor; 3) substituting the substrate binding parameters with corresponding calculated values from **Table 1**; 4) substituting V_{max} parameters for 2800 and 1600 pmol/min/mg protein for EROD and MROD respectively. The calculated EROD/MROD activity ratio using this approach was 8.1 times for CYP1A1, in good agreement with the published data. The same ratio for CYP1A2 calculated by **Eq. 2** and **Eq. 5** and using V_{max} values of 1909 and 1969 pmol/min/mg protein for EROD and MROD respectively resulted in an activity ratio of 1.64, suggesting a decreased CYP1A2 preference for MROD in mouse liver microsomes compared to the reconstituted recombinant enzyme system. It should be noted that at 0.5 μM MR the calculated EROD/MROD activity ratio was 0.63 suggesting a higher CYP1A2 preference for MROD at low substrate concentrations. However, at high substrate concentrations the ratio changes, possibly due to substrate inhibition.

Microsomal stability of ramelteon and tacrine

The CYP1A2-specific substrate ramelteon exhibited mono-exponential decay on incubation with liver microsomes from all vehicle treated samples and HLM (**Figure 8A**). Ramelteon *in vitro* clearance in Cyp1a KO and hCYP1A1/1A2 mice and pooled human liver microsomes was ~83%, ~190% and ~70% relative to WT animals (**Figure 8C**). The values of the fraction metabolised by Cyp1a2/CYP1A2 were calculated to be ~0.17 and 0.56 for WT and hCYP1A1/1A2 mice, respectively (**Eq. 15-16**). Tacrine depletion was mono-exponential in all samples except Cyp1a KO microsomes which was preferentially described by double exponential decay equation (**Figure 8B**). The *in vitro* clearance of tacrine in pooled human liver microsomes was only ~12% of that in WT mice and in microsomes from Cyp1a KO and hCYP1A1/1A2 mice it was ~32% and 81% of that in WT animals respectively (**Figure 8D**). The calculated Cyp1a2/CYP1A2 fraction metabolised values were ~0.68 and ~0.60 for WT and hCYP1A1/1A2 mice, respectively (**Eq. 15-16**).

Caffeine pharmacokinetics

Caffeine is a CYP1A2-specific substrate, recommended by the FDA as a sensitive "substrate drug" for *in vivo* CYP1A2 drug-drug interaction studies. We therefore studied caffeine pharmacokinetics in hCYP1A1/1A2 and Cyp1a KO mice. The pharmacokinetics of caffeine had similar absorption phases in all mouse lines (**Figure 9**). There was a small increase (<1.7-fold) in the maximum observed concentration and a minor (<21%) decrease in the apparent volume of distribution in Cyp1a KO, hCYP1A1/1A2 and HRN mice compared to the WT animals (**Figure 9**; **Table 2**). In Hepatic Reductase Null (HRN) and Cyp1a KO mice the elimination half-life was significantly increased (~8.9- and ~2.5-fold, respectively) compared to that measured in the WT. In hCYP1A1/1A2 mice the increase was small (~1.4-fold) and not statistically significant. The AUC values were significantly increased (~10-, ~3.1- and ~1.5-fold compared to WT mice) and apparent clearance values were significantly decreased (to ~10%, 32% and 68% of that in WT mice) in HRN, Cyp1a KO and hCYP1A1/1A2 mice, respectively.

Caffeine pharmacokinetics in hCYP1A1/1A2, Cyp1a KO and HRN mice were extrapolated to those in man by complex Dedrick plot approach using body weight, clearance and volume of distribution values in man obtained from Culm-Merdek (Culm-Merdek et al., 2005) and hCYP1A1/1A2 mice to calculate parameters of exponential functions relating clearance and volume of distribution to body weight (**Figure 10**; see **Supplemental Data**). The data extrapolated from the different mouse lines were compared to caffeine pharmacokinetics observed in healthy human subjects who received placebo or fluvoxamine, a strong CYP1A2 inhibitor (Culm-Merdek et al., 2005). The extrapolated caffeine pharmacokinetics in hCYP1A1/1A2 mice superimposed with that in humans receiving a placebo, whilst the extrapolated trace from HRN mice was close to that measured in human subjects after co-administration of caffeine and fluvoxamine. Caffeine pharmacokinetics extrapolated from Cyp1a KO mice demonstrated slower elimination than that in man with placebo but faster compared to that in healthy subjects after co-administration of fluvoxamine.

Discussion

We have generated and validated two new mouse models, one where the *Cyp1a* gene cluster has been deleted and one humanised for CYP1A1 and CYP1A2. These models have been used to develop a novel approach to establish the relative roles of CYP1A1 and CYP1A2 in drug disposition. Both CYP1A1 and CYP1A2 are induced as a consequence of the activation of the Ah receptor and their overlapping substrate specificities has led to considerable interest in developing methods to distinguish their relative contribution to drug oxidation *in vitro* and *in vivo*. One approach has been to use selective CYP1A2 inhibitors, such as fluvoxamine/isosafrole (Pastrakuljic et al., 1997; Sy et al., 2001) or furafylline (Stiborova et al., 2002; Stiborova et al., 2005). Recombinant CYP1A1 and CYP1A2 were used to establish the ratio of activities with isosafrole or fluvoxamine to that without the inhibitor at a single substrate and a number of inhibitor concentrations (Pastrakuljic et al., 1997). Thus, for each inhibitor concentration there was one ratio for CYP1A1 and one ratio for CYP1A2. The activity in a sample of human liver microsomes was measured with and without the inhibitor and an equation relating the activities measured in human liver microsomes to the activity ratios in the recombinant enzymes used to calculate the individual contribution of CYP1A1 and CYP1A2. However, the method has the shortcoming that it uses a single substrate concentration and a limited number of inhibitor concentrations and thus does not use the full magnitude of the kinetic data collected. The latter method (Stiborova et al., 2002; Stiborova et al., 2005) relies on subtracting activity measured in the presence of furafylline from that without the inhibitor and relating the difference to CYP1A1 concentration measured in human liver microsomes by Western blotting. Whilst the method worked for compounds rapidly metabolised by CYP1A1 e.g. Sudan I, in the case of EROD the approach did not work. Incomplete inhibition of CYP1A2 and contribution from other cytochromes P450 participating in EROD in the presence of furafylline were considered as possible explanations (Stiborova et al., 2005).

The present study exploits the Cyp1a KO model together with quinidine as a specific CYP1A1 inhibitor to define the relative role of CYP1A1/1A2 in drug metabolism, using EROD and MROD as exemplar substrates. Our approach involved the derivation of equations to describe the relationship between reaction rate and substrate and inhibitor concentrations in liver microsomes from hCYP1A1/1A2 mice. This mechanistic approach allows modelling of the CYP1A1, CYP1A2 and non-CYP1A contribution to metabolism of any substrate, at any substrate, inhibitor or enzyme concentration and thus can be easily integrated to a PBPK model. Through the use of quinidine as a CYP1A1-specific inhibitor the CYP1A1 contribution to metabolism of compounds with a slow reaction rate or where CYP1A1 expression is low can be determined.

Hepatic CYP1A1 expression in man has been reported to be undetectable (McManus et al., 1990; Murray et al., 1993; Edwards et al., 1998; Edwards et al., 2003) while others have quantified the enzyme (Drahushuk et al., 1998; Stiborova et al., 2005). The individual contribution of CYP1A1 and CYP1A2 to EROD in a panel of human microsomes has been estimated by selective inhibition of CYP1A2 and CYP1A1 (Pastrakuljic et al., 1997; Sy et al., 2001). In all human samples the CYP1A1 content was either very low, estimated to be <0.7% of the total hepatic cytochrome P450 (Stiborova et al., 2005), or below the limit of detection inferring that hepatic CYP1A1 is induced rather than constitutive (Sy et al., 2001). However, due to the very high activity of CYP1A1 towards some compounds (Roberts-Thomson et al., 1993; Kreth et al., 2000; Stiborova et al., 2005; Li et al., 2007; Stiborova et al., 2015; Lin et al., 2017; MacLeod et al., 2018) it can make a significant contribution to their metabolism even at a very low expression levels, for example, aristolochic acid (Stiborova et al., 2015), Sudan I (Stiborova et al., 2005), benzo[a]pyrene (Sulc et al., 2016), granisetron (Nakamura et al., 2005), riociguat (Khaybullina et al., 2014) and erlotinib (Hamilton et al., 2006).

Whilst the measured concentration of CYP1A1 in human liver microsomes is very low (≤3 pmol/mg microsomal protein (Stiborova et al., 2005)), it is inducible in cultured human hepatocytes (Curi-Pedrosa et al., 1994; Liu et al., 2001) and in human liver slices, where

following incubation with TCDD an expression level of 25-50 pmol/mg microsomal protein was measured (Drahushuk et al., 1998). The combination of high activity and inducibility makes CYP1A1 a potentially important contributor to variability in toxico/pharmacokinetics of environmental toxicants and/or approved drugs. Indeed, the enzyme can not only be induced by environmental agents but also by prescribed drugs such as omeprazole, lansoprazole, albendazole and primaquine (Curi-Pedrosa et al., 1994; Krusekopf et al., 2003; Ueda et al., 2006; Thorn et al., 2012).

In this study recombinant CYP1A1 metabolised ER with a V_{max} of 3300 pmol/min/mg protein at an enzyme concentration 71 pmol/mg protein, giving a k_{cat} of 47 min^{-1}. The concentration of hepatic CYP1A1 in TCDD-treated hCYP1A1/1A2 mice, estimated from the ratio of CYP1A1 EROD V_{max} (2800 pmol/min/mg protein) to k_{cat} (47 min^{-1}), is 59 pmol/mg microsomal protein. This is in reasonable agreement with the CYP1A1 concentration range of 25-50 pmol/min/mg microsomal protein, obtained in human liver slices incubated with TCDD (Drahushuk et al., 1998), suggesting that any variability in CYP1A1 activity due to induction can be modelled in hCYP1A1/1A2 mice and its relation to variability in pharmacokinetics of any given drug modelled and tested.

CYP1A2 in untreated humanised mice had a much higher activity than Cyp1a2 in the oxidation of ramelteon. Indeed, the contribution of mouse Cyp1a2 to clearance of this substrate was only 17%, whilst in the liver microsomes of hCYP1A1/1A2 mice it was increased to 56%, close to that observed in human liver microsomes *in vitro* (Obach and Ryder, 2010). Similarly, CYP1A2 exhibited a higher EROD activity than Cyp1a2. The MROD efficacy of both enzymes was similar whilst tacrine oxidation was faster in liver microsomes from C57BL/6J mice compared to that in the humanized animals. These observations highlight and substantiate the reported species differences in the metabolism of various CYP1A2/Cyp1a2 substrates (Turesky et al., 1998).

The contribution of Cyp1a2 and CYP1A2 to caffeine clearance in WT or hCYP1A1/1A2 was 68% and 53%, respectively (**Table 3**), suggesting that the mouse enzyme plays a slightly greater role in caffeine disposition. The Cyp1a2 contribution was lower than the 87% established using a Cyp1a2 knock-out model (Buters et al., 1996). However, as shown in **Table 3**, the clearance values for the WT mouse in the Buters study was abnormally high and the clearance measured in the Cyp1a KO mouse was the same. In this study we demonstrate the power of using the Cyp1aKO in conjunction with the humanised mouse to clearly establish the contribution of a particular enzyme in drug elimination. This is important in the study of drug/drug interactions (**Figure 11**). At an inhibitor concentration of 10 times Ki, where the contribution of the enzyme to elimination is 87%, the “substrate drug” AUC will increase approximately 5-fold. This would be considered a strong drug/drug interaction. However, with a 68% enzyme contribution to the drug clearance the AUC will only increase approximately 2.5-fold, corresponding to a moderate interaction. For a 53% enzyme contribution the AUC increase will be less than 2-fold and be a weak effect. The interaction of caffeine with fluvoxamine, a strong CYP1A2 inhibitor, suggested a 93% contribution of CYP1A2 to caffeine metabolism in healthy subjects (Culm-Merdek et al., 2005).

When caffeine pharmacokinetics in hCYP1A1/1A2 mice was extrapolated to man, as described in the Materials and Methods, the PK curves were almost identical (**Figure 10**). In the case of Cyp1a KO mice, which have no hepatic CYP1A2 activity, and therefore comparable to man when CYP1A2 is completely inhibited, the extrapolated curve from the null mice suggested notably faster caffeine elimination than that observed in individuals co-administered with the CYP1A2 inhibitor fluvoxamine. However, caffeine elimination extrapolated from HRN mice was superimposable with the fluvoxamine-treated group, suggesting the involvement of P450s other than Cyp1a2 in metabolism. Although this could be considered a confounding factor in the use of the model, it also demonstrates how the model can identify other enzymes involved in drug disposition. A contribution of the murine enzymes to the fraction metabolised is likely to be reduced using the more complex

humanised model we have reported recently. In this model 32 murine P450s from four gene subfamilies have been deleted and substituted for the major human P450s involved in foreign compound metabolism, along with CAR and PXR, the major transcription factors involved in their regulation (Henderson et al., 2019).

The mechanistic approach developed in this study was successfully applied to calculate the individual contribution of human CYP1A1 and CYP1A2 to the metabolism of model compounds 7-ER and 7-MR in liver microsomes from TCDD-treated hCYP1A1/1A2 mice. When applied to a new chemical entity the method will provide data for the development of a PBPK model, and the predicted interplay between compound concentration and expression of CYP1A1 and CYP1A2 can be tested *in vivo* using hCYP1A1/1A2 and Cyp1a KO mice. This represents a significant improvement on the currently used *in vitro* approaches as it allows the validity of models to be tested *in vivo*. Humanisation for CYP1A1 and CYP1A2, and particularly the use of complex humanised models such as that reported recently (Henderson et al., 2019) will improve the accuracy of extrapolation of preclinical data to man.

Acknowledgements

The assistance of Julia Carr, Dr Kenneth MacLeod and Tanya Frangova with animal work is gratefully acknowledged.

Authorship Contributions

Participated in research design: Kapelyukh, Henderson, Wolf

Conducted experiments: Kapelyukh, Henderson,

Contributed new reagents or analytic tools: Scheer, Rode, Kapelyukh, Henderson, Wolf

Performed data analysis: Kapelyukh, Henderson, Wolf

Wrote or contributed to the writing of the manuscript: Kapelyukh, Henderson, Scheer, Rode, Wolf

References

Abraham K, Geusau A, Tosun Y, Helge H, Bauer S, and Brockmoller J (2002) Severe 2,3,7,8-tetrachlorodibenzo-p-dioxin (TCDD) intoxication: insights into the measurement of hepatic cytochrome P450 1A2 induction. *Clin Pharmacol Ther* **72:**163-174.

Achour B, Barber J, and Rostami-Hodjegan A (2014) Expression of hepatic drug-metabolizing cytochrome p450 enzymes and their intercorrelations: a meta-analysis. *Drug Metab Dispos* **42:**1349-1356.

Andersen ME, Birnbaum LS, Barton HA, and Eklund CR (1997) Regional hepatic CYP1A1 and CYP1A2 induction with 2,3,7,8-tetrachlorodibenzo-p-dioxin evaluated with a multicompartment geometric model of hepatic zonation. *Toxicol Appl Pharmacol* **144:**145-155.

Behringer R, Gertsenstein M, Nagy KV, and Nagy A (2014) Manipulating the Mouse Embryo - A Laboratory Manual. *Cold Spring Harbor Laboratory Press* **Fourth Edition:**321-485.

Burke MD, Thompson S, Weaver RJ, Wolf CR, and Mayer RT (1994) Cytochrome P450 specificities of alkoxyresorufin O-dealkylation in human and rat liver. *Biochem Pharmacol* **48:**923-936.

Buters JT, Tang BK, Pineau T, Gelboin HV, Kimura S, and Gonzalez FJ (1996) Role of CYP1A2 in caffeine pharmacokinetics and metabolism: studies using mice deficient in CYP1A2. *Pharmacogenetics* **6:**291-296.

Cheung C and Gonzalez FJ (2008) Humanized mouse lines and their application for prediction of human drug metabolism and toxicological risk assessment. *J Pharmacol Exp Ther* **327:**288-299.

Cheung C, Ma X, Krausz KW, Kimura S, Feigenbaum L, Dalton TP, Nebert DW, Idle JR, and Gonzalez FJ (2005) Differential metabolism of 2-amino-1-methyl-6-phenylimidazo[4,5-

b]pyridine (PhIP) in mice humanized for CYP1A1 and CYP1A2. *Chem Res Toxicol* **18:**1471-1478.

Ching MS, Blake CL, Malek NA, Angus PW, and Ghabrial H (2001) Differential inhibition of human CYP1A1 and CYP1A2 by quinidine and quinine. *Xenobiotica* **31:**757-767.

Corchero J, Pimprale S, Kimura S, and Gonzalez FJ (2001) Organization of the CYP1A cluster on human chromosome 15: implications for gene regulation. *Pharmacogenetics* **11:**1-6.

Cortessis V and Thomas DC (2004) Toxicokinetic genetics: an approach to gene-environment and gene-gene interactions in complex metabolic pathways. *IARC Sci Publ***:**127-150.

Culm-Merdek KE, von Moltke LL, Harmatz JS, and Greenblatt DJ (2005) Fluvoxamine impairs single-dose caffeine clearance without altering caffeine pharmacodynamics. *Br J Clin Pharmacol* **60:**486-493.

Curi-Pedrosa R, Daujat M, Pichard L, Ourlin JC, Clair P, Gervot L, Lesca P, Domergue J, Joyeux H, Fourtanier G, and et al. (1994) Omeprazole and lansoprazole are mixed inducers of CYP1A and CYP3A in human hepatocytes in primary culture. *J Pharmacol Exp Ther* **269:**384-392.

Drahushuk AT, McGarrigle BP, Larsen KE, Stegeman JJ, and Olson JR (1998) Detection of CYP1A1 protein in human liver and induction by TCDD in precision-cut liver slices incubated in dynamic organ culture. *Carcinogenesis* **19:**1361-1368.

Edwards RJ, Adams DA, Watts PS, Davies DS, and Boobis AR (1998) Development of a comprehensive panel of antibodies against the major xenobiotic metabolising forms of cytochrome P450 in humans. *Biochem Pharmacol* **56:**377-387.

Edwards RJ, Price RJ, Watts PS, Renwick AB, Tredger JM, Boobis AR, and Lake BG (2003) Induction of cytochrome P450 enzymes in cultured precision-cut human liver slices. *Drug Metab Dispos* **31:**282-288.

Floreani M, Gabbia D, Barbierato M, S DEM, and Palatini P (2012) Differential inducing effect of benzo[a]pyrene on gene expression and enzyme activity of cytochromes P450 1A1 and 1A2 in Sprague-Dawley and Wistar rats. *Drug Metab Pharmacokinet* **27:**640-652.

Forrester LM, Henderson CJ, Glancey MJ, Back DJ, Park BK, Ball SE, Kitteringham NR, McLaren AW, Miles JS, Skett P, and et al. (1992) Relative expression of cytochrome P450 isoenzymes in human liver and association with the metabolism of drugs and xenobiotics. *Biochem J* **281 (Pt 2):**359-368.

Hamilton M, Wolf JL, Rusk J, Beard SE, Clark GM, Witt K, and Cagnoni PJ (2006) Effects of smoking on the pharmacokinetics of erlotinib. *Clin Cancer Res* **12:**2166-2171.

Henderson CJ, Kapelyukh Y, Scheer N, Rode A, McLaren AW, MacLeod AK, Lin, Wright J, Stanley L, and Wolf CR (2019) An extensively humanised mouse model to predict pathways of drug disposition, drug/drug interactions, and to facilitate the design of clinical trials. *Drug Metab Dispos* **47:**601-615.

Henderson CJ, Otto DM, Carrie D, Magnuson MA, McLaren AW, Rosewell I, and Wolf CR (2003) Inactivation of the hepatic cytochrome P450 system by conditional deletion of hepatic cytochrome P450 reductase. *J Biol Chem* **278:**13480-13486.

Iwatsubo T, Hirota N, Ooie T, Suzuki H, Shimada N, Chiba K, Ishizaki T, Green CE, Tyson CA, and Sugiyama Y (1997) Prediction of in vivo drug metabolism in the human liver from in vitro metabolism data. *Pharmacol Ther* **73:**147-171.

Kakkar T, Pak Y, and Mayersohn M (2000) Evaluation of a minimal experimental design for determination of enzyme kinetic parameters and inhibition mechanism. *J Pharmacol Exp Ther* **293:**861-869.

Kaplan GB, Tai NT, Greenblatt DJ, and Shader RI (1990) Caffeine-induced behavioural stimulation is dose- and concentration-dependent. *Br J Pharmacol* **100:**435-440.

Khaybullina D, Patel A, and Zerilli T (2014) Riociguat (adempas): a novel agent for the treatment of pulmonary arterial hypertension and chronic thromboembolic pulmonary hypertension. *P T* **39:**749-758.

Kreth K, Kovar K, Schwab M, and Zanger UM (2000) Identification of the human cytochromes P450 involved in the oxidative metabolism of "Ecstasy"-related designer drugs. *Biochem Pharmacol* **59:**1563-1571.

Krusekopf S, Roots I, Hildebrandt AG, and Kleeberg U (2003) Time-dependent transcriptional induction of CYP1A1, CYP1A2 and CYP1B1 mRNAs by H+/K+ -ATPase inhibitors and other xenobiotics. *Xenobiotica* **33:**107-118.

Levova K, Moserova M, Nebert DW, Phillips DH, Frei E, Schmeiser HH, Arlt VM, and Stiborova M (2012) NAD(P)H:quinone oxidoreductase expression in Cyp1a-knockout and CYP1A-humanized mouse lines and its effect on bioactivation of the carcinogen aristolochic acid I. *Toxicol Appl Pharmacol* **265:**360-367.

Li H, Clarke JD, Dzierlenga AL, Bear J, Goedken MJ, and Cherrington NJ (2017) In vivo cytochrome P450 activity alterations in diabetic nonalcoholic steatohepatitis mice. *J Biochem Mol Toxicol* **31**.

Li J, Zhao M, He P, Hidalgo M, and Baker SD (2007) Differential metabolism of gefitinib and erlotinib by human cytochrome P450 enzymes. *Clin Cancer Res* **13:**3731-3737.

Lin, Kostov R, Huang JT, Henderson CJ, and Wolf CR (2017) Novel Pathways of Ponatinib Disposition Catalyzed By CYP1A1 Involving Generation of Potentially Toxic Metabolites. *J Pharmacol Exp Ther* **363:**12-19.

Liu J, Ericksen SS, Sivaneri M, Besspiata D, Fisher CW, and Szklarz GD (2004) The effect of reciprocal active site mutations in human cytochromes P450 1A1 and 1A2 on alkoxyresorufin metabolism. *Arch Biochem Biophys* **424:**33-43.

Liu N, Zhang QY, Vakharia D, Dunbar D, and Kaminsky LS (2001) Induction of CYP1A by benzo[k]fluoranthene in human hepatocytes: CYP1A1 or CYP1A2? *Arch Biochem Biophys* **389:**130-134.

Lowry OH, Rosebrough NJ, Farr AL, and Randall RJ (1951) Protein measurement with the Folin phenol reagent. *J Biol Chem* **193:**265-275.

MacLeod AK, Lin, Huang JT, McLaughlin LA, Henderson CJ, and Wolf CR (2018) Identification of Novel Pathways of Osimertinib Disposition and Potential Implications for the Outcome of Lung Cancer Therapy. *Clin Cancer Res* **24:**2138-2147.

McGinnity DF, Griffin SJ, Moody GC, Voice M, Hanlon S, Friedberg T, and Riley RJ (1999) Rapid characterization of the major drug-metabolizing human hepatic cytochrome P-450 enzymes expressed in Escherichia coli. *Drug Metab Dispos* **27:**1017-1023.

McManus ME, Burgess WM, Veronese ME, Huggett A, Quattrochi LC, and Tukey RH (1990) Metabolism of 2-acetylaminofluorene and benzo(a)pyrene and activation of food-derived heterocyclic amine mutagens by human cytochromes P-450. *Cancer Res* **50:**3367-3376.

Murray BP, Edwards RJ, Murray S, Singleton AM, Davies DS, and Boobis AR (1993) Human hepatic CYP1A1 and CYP1A2 content, determined with specific anti-peptide antibodies, correlates with the mutagenic activation of PhIP. *Carcinogenesis* **14:**585-592.

Nakamura H, Ariyoshi N, Okada K, Nakasa H, Nakazawa K, and Kitada M (2005) CYP1A1 is a major enzyme responsible for the metabolism of granisetron in human liver microsomes. *Curr Drug Metab* **6:**469-480.

Namkung MJ, Yang HL, Hulla JE, and Juchau MR (1988) On the substrate specificity of cytochrome P450IIIA1. *Mol Pharmacol* **34:**628-637.

Nebert DW, Shi Z, Galvez-Peralta M, Uno S, and Dragin N (2013) Oral benzo[a]pyrene: understanding pharmacokinetics, detoxication, and consequences--Cyp1 knockout mouse lines as a paradigm. *Mol Pharmacol* **84:**304-313.

Obach RS and Ryder TF (2010) Metabolism of ramelteon in human liver microsomes and correlation with the effect of fluvoxamine on ramelteon pharmacokinetics. *Drug Metab Dispos* **38:**1381-1391.

Omura T and Sato R (1964) THE CARBON MONOXIDE-BINDING PIGMENT OF LIVER MICROSOMES. I. EVIDENCE FOR ITS HEMOPROTEIN NATURE. *J Biol Chem* **239:**2370-2378.

Pastrakuljic A, Tang BK, Roberts EA, and Kalow W (1997) Distinction of CYP1A1 and CYP1A2 activity by selective inhibition using fluvoxamine and isosafrole. *Biochem Pharmacol* **53:**531-538.

Roberts-Thomson SJ, McManus ME, Tukey RH, Gonzalez FF, and Holder GM (1993) The catalytic activity of four expressed human cytochrome P450s towards benzo[a]pyrene and the isomers of its proximate carcinogen. *Biochem Biophys Res Commun* **192:**1373-1379.

Samojlik I, Petkovic S, Stilinovic N, Vukmirovic S, Mijatovic V, and Bozin B (2016) Pharmacokinetic Herb-Drug Interaction between Essential Oil of Aniseed (Pimpinella anisum L., Apiaceae) and Acetaminophen and Caffeine: A Potential Risk for Clinical Practice. *Phytother Res* **30:**253-259.

Sansen S, Yano JK, Reynald RL, Schoch GA, Griffin KJ, Stout CD, and Johnson EF (2007) Adaptations for the oxidation of polycyclic aromatic hydrocarbons exhibited by the structure of human P450 1A2. *J Biol Chem* **282:**14348-14355.

Santostefano MJ, Wang X, Richardson VM, Ross DG, DeVito MJ, and Birnbaum LS (1998) A pharmacodynamic analysis of TCDD-induced cytochrome P450 gene expression in multiple tissues: dose- and time-dependent effects. *Toxicol Appl Pharmacol* **151:**294-310.

Scheer N, Kapelyukh Y, Chatham L, Rode A, Buechel S, and Wolf CR (2012a) Generation and characterization of novel cytochrome P450 Cyp2c gene cluster knockout and CYP2C9 humanized mouse lines. *Mol Pharmacol* **82:**1022-1029.

Scheer N, Kapelyukh Y, McEwan J, Beuger V, Stanley LA, Rode A, and Wolf CR (2012b) Modeling human cytochrome P450 2D6 metabolism and drug-drug interaction by a novel panel of knockout and humanized mouse lines. *Mol Pharmacol* **81:**63-72.

Scheer N, McLaughlin LA, Rode A, Macleod AK, Henderson CJ, and Wolf CR (2014) Deletion of 30 murine cytochrome p450 genes results in viable mice with compromised drug metabolism. *Drug Metab Dispos* **42:**1022-1030.

Shinkyo R, Sakaki T, Ohta M, and Inouye K (2003) Metabolic pathways of dioxin by CYP1A1: species difference between rat and human CYP1A subfamily in the metabolism of dioxins. *Arch Biochem Biophys* **409:**180-187.

Stiborova M, Barta F, Levova K, Hodek P, Schmeiser HH, Arlt VM, and Martinek V (2015) A Mechanism of O-Demethylation of Aristolochic Acid I by Cytochromes P450 and Their Contributions to This Reaction in Human and Rat Livers: Experimental and Theoretical Approaches. *Int J Mol Sci* **16:**27561-27575.

Stiborova M, Frei E, Arlt VM, and Schmeiser HH (2014) Knockout and humanized mice as suitable tools to identify enzymes metabolizing the human carcinogen aristolochic acid. *Xenobiotica* **44:**135-145.

Stiborova M, Martinek V, Rydlova H, Hodek P, and Frei E (2002) Sudan I is a potential carcinogen for humans: evidence for its metabolic activation and detoxication by human recombinant cytochrome P450 1A1 and liver microsomes. *Cancer Res* **62:**5678-5684.

Stiborova M, Martinek V, Rydlova H, Koblas T, and Hodek P (2005) Expression of cytochrome P450 1A1 and its contribution to oxidation of a potential human carcinogen 1-phenylazo-2-naphthol (Sudan I) in human livers. *Cancer Lett* **220:**145-154.

Sulc M, Indra R, Moserova M, Schmeiser HH, Frei E, Arlt VM, and Stiborova M (2016) The impact of individual cytochrome P450 enzymes on oxidative metabolism of benzo[a]pyrene in human livers. *Environ Mol Mutagen* **57:**229-235.

Sy SK, Tang BK, Pastrakuljic A, Roberts EA, and Kalow W (2001) Detailed characterization of experimentally derived human hepatic CYP1A1 activity and expression using differential inhibition of ethoxyresorufin O-deethylation by fluvoxamine. *Eur J Clin Pharmacol* **57:**377-386.

Thorn CF, Aklillu E, Klein TE, and Altman RB (2012) PharmGKB summary: very important pharmacogene information for CYP1A2. *Pharmacogenet Genomics* **22:**73-77.

Turesky RJ, Constable A, Richoz J, Varga N, Markovic J, Martin MV, and Guengerich FP (1998) Activation of heterocyclic aromatic amines by rat and human liver microsomes and by purified rat and human cytochrome P450 1A2. *Chem Res Toxicol* **11:**925-936.

Turteltaub KW, Dingley KH, Curtis KD, Malfatti MA, Turesky RJ, Garner RC, Felton JS, and Lang NP (1999) Macromolecular adduct formation and metabolism of heterocyclic amines in humans and rodents at low doses. *Cancer Lett* **143:**149-155.

Ueda R, Iketaki H, Nagata K, Kimura S, Gonzalez FJ, Kusano K, Yoshimura T, and Yamazoe Y (2006) A common regulatory region functions bidirectionally in transcriptional activation of the human CYP1A1 and CYP1A2 genes. *Mol Pharmacol* **69:**1924-1930.

Walsh AA, Szklarz GD, and Scott EE (2013) Human cytochrome P450 1A1 structure and utility in understanding drug and xenobiotic metabolism. *J Biol Chem* **288:**12932-12943.

Walton K, Dorne JL, and Renwick AG (2001) Uncertainty factors for chemical risk assessment: interspecies differences in the in vivo pharmacokinetics and metabolism of human CYP1A2 substrates. *Food Chem Toxicol* **39:**667-680.

Yoshinari K, Ueda R, Kusano K, Yoshimura T, Nagata K, and Yamazoe Y (2008) Omeprazole transactivates human CYP1A1 and CYP1A2 expression through the common regulatory region containing multiple xenobiotic-responsive elements. *Biochem Pharmacol* **76:**139-145.

Yoshinari K, Yoda N, Toriyabe T, and Yamazoe Y (2010) Constitutive androstane receptor transcriptionally activates human CYP1A1 and CYP1A2 genes through a common regulatory element in the 5'-flanking region. *Biochem Pharmacol* **79:**261-269.

Footnotes

Financial support: This research was supported by a Cancer Research UK Programme Grant [C4639/A10822] and Medical Research Council Project Grant MR/R017506/1.

Figure legends

Figure 1: Total cytochrome P450 in liver microsomes from vehicle and TCDD-treated WT, hCYP1A1/1A2 and Cyp1a KO mice

Liver microsomes were prepared from vehicle (corn-oil) and TCDD-treated hCYP1A1/1A2, Cyp1a KO and WT mice (n=4) and total cytochrome P450 content measured as detailed in Materials and Methods. Data are presented as mean ± SD; ** - significantly different from corresponding corn oil-treated group (unpaired t-test; two-tailed p value; $p<0.01$).

Figure 2: Basal and TCDD-inducible expression of Cyp1a/CYP1A in tissues from WT, Cyp1a KO and hCYP1A1/1A2 mice

Microsomes were prepared from vehicle (corn-oil) and TCDD-treated hCYP1A1/1A2, Cyp1a KO and WT mice from the tissues shown and immunoblotted for hCYP1A1 (**A, D**), human CYP1A2 (**B**) and mouse Cyp1a (**C**) as detailed in Materials & Methods.

Standards: CYP1A1 (0.36 pmol/lane) and CYP1A2 (1 pmol/lane) expressed in bacterial membranes

Figure 3: EROD and MROD activities in hepatic and extra-hepatic tissues from WT, Cyp1a KO and hCYP1A1/1A2 mice

Liver microsomes were prepared from vehicle (corn-oil) and TCDD-treated hCYP1A1/1A2, Cyp1a KO and WT mice for the tissues shown and EROD (**A**) and MROD (**B**) activities measured as detailed in Materials & Methods. Microsomes from extra-hepatic tissues of TCDD-treated hCYP1A1/1A2 and WT mice were prepared and EROD (**C**) and MROD (**D**) activities measured.

Data are presented as mean ± SD (n=4). * - significantly different from corresponding WT group (unpaired t-test; two-tailed p-value; **- $p<0.01$; ***- $p<0.001$; ****- $p<0.0001$). Heart, lung, spleen, kidney, brain and testis microsomes were prepared from pooled organs of each experimental group. Their activities are presented as mean ± SD of three measurements of

the pooled sample. No test for statistical significance was performed on these data. HLM = pooled human liver microsomes.

Figure 4: Effect of quinidine on MROD activity catalysed by recombinant human CYP1A1 and CYP1A2

Recombinant human CYP1A1 (closed circles) and CYP1A2 (open circles) were co-expressed with human P450 reductase in bacterial microsomes and activity measured as detailed in Materials and Methods.

Figure 5: Effect of quinidine on EROD and MROD activities catalysed by recombinant human CYP1A1, CYP1A2 and liver microsomes from Cyp1a KO mice at different substrate concentrations

EROD (**A, C, E**) and MROD (**B, D, F**) catalysed by recombinant human CYP1A1 (**A, B**); CYP1A2 (**C, D**) and liver microsomes from TCDD-treated Cyp1a KO mice (**E, F**) at different concentrations of substrate and quinidine as detailed in Materials and Methods. Symbols are the measured reaction rates. Lines are non-linear regression analysis of the data using **Eq. 1-6** (for details see **Data Analysis** in **Supplemental Data**).

Figure 6: EROD and MROD activities measured in the presence or absence of quinidine in liver microsomes from TCDD-treated hCYP1A1/1A2 humanised mice

EROD (**A**) and MROD (**B**) with and without quinidine catalysed by liver microsomes from TCDD treated hCYP1A1/1A2 humanised mice. Symbols are the measured reaction rates. Lines are non-linear regression analysis of the data using **Eq. 7 & 8**, respectively (for details see **Data Analysis**). Contribution of CYP1A1, CYP1A2 and non-CYP1A components of the reactions were calculated using equations 9 – 14 (for details see **Data Analysis** in **Supplemental Data**) for EROD (**C, E**) and MROD (**D, F**) with (**E, F**) and without (**C, D**) quinidine (200 μM).

Figure 7: **EROD and MROD activities catalysed by liver microsomes from vehicle-treated hCYP1A1/1A2 humanised mice in the presence or absence of quinidine**

EROD (**A**) and MROD (**B**) with and without quinidine catalysed by liver microsomes from vehicle-(corn oil) treated hCYP1A1/1A2 humanised mice. Symbols are the measured reaction rates and the line is derived from non-linear regression analysis of the MROD in the absence of quinidine using **Eq. 5** (for details see **Data Analysis** in **Supplemental Data**).

Figure 8: **Microsomal stability and *in vitro* clearance of ramelteon and tacrine**

Microsomal stability (**A, B**) and in vitro clearance (**C, D**) of human CYP1A2 substrates ramelteon (a and c) and tacrine (b and d) measured in liver microsomes from WT, Cyp1a KO and hCYP1A1/1A2 mice and human donors (HLM). Symbols are the measured concentrations of the compounds. A no NADPH control was also run. Lines are non-linear regression analysis using the equation for double exponential (tacrine with Cyp1a KO microsomes) or mono exponential (all other incubations) decay in the software package GraFit 7.0.3. (Erithacus, UK).

Figure 9: Caffeine pharmacokinetics in WT, Cyp1a KO, hCYP1A1/1A2 and HRN mice

Symbols are caffeine concentrations measured in mouse whole blood. All data are expressed as mean ± S.D. (n = 4 mice per treatment group).

Figure 10: Caffeine pharmacokinetics in hCYP1A1/1A2, Cyp1a KO and HRN mice extrapolated to human

Caffeine pharmacokinetics in hCYP1A1/1A2, Cyp1a KO and HRN mice extrapolated to human using the complex Dedrick plot approach (see Materials and Methods for details). The caffeine concentration time-course in placebo- or fluvoxamine-treated healthy subjects (Culm-Merdek et al., 2005) was corrected for mean caffeine concentration in pre-dose. Symbols are the corrected caffeine concentrations measured in human plasma or extrapolated from mouse

whole blood. All data are expressed as mean values (n = 4 mice per treatment group; n=7 healthy subjects per treatment group).

Figure 11: Effect of fraction metabolised on AUC ratios of "substrate drug"

Simulation of AUC ratios of a "substrate drug" with inhibitor to that without inhibitor as a function of inhibitor concentration for different contribution of the inhibited enzyme (fraction metabolized (f_m)) to the "substrate drug' elimination. The enzyme contribution is expressed as part of total clearance. Horizontal lines separate areas with strong (AUC ratio >5-fold), moderate (2< AUC ratio <5), weak (1.25<AUC ratio<2) and "no effect" (AUC ratio <1.25-fold) inhibition.

DMD Fast Forward. Published on May 30, 2019 as DOI: 10.1124/dmd.119.087718
This article has not been copyedited and formatted. The final version may differ from this version.

Tables

Table 1: Kinetic parameters of EROD and MROD inhibition by quinidine in microsomes

Microsomes origin	K_{s1} ±SE μM	K_{s2} ±SE μM	K_i ±SE μM	α	Quinidine inhibition type
			EROD		
rCYP1A1	0.09±0.008	11±1	3.3±0.35	31±8	Mixed
rCYP1A2	(Km)1.2±0.2	NA	NA	NA	NA
Cyp1a KO	0.83±0.04	13±1.5	422±18	NA	Non-competitive
			MROD		
rCYP1A1	0.47±0.07	1.3±0.18	2.2±0.18	NA	Competitive
rCYP1A2	0.58±0.08	12±3.5	NA	NA	NA
Cyp1a KO	0.96±0.18	3.4±0.8	272±28	NA	Non-competitive

K_{s1} is a dissociation constant of the productive enzyme-substrate complex; K_{s2} is a dissociation constant of the inhibitory enzyme-substrate complex; K_i is a dissociation constant of the enzyme-inhibitor complex; α is a parameter describing the effect of inhibitor binding on the binding of the substrate and vice versa; NA = not applicable

Table 2: Caffeine pharmacokinetics parameters in hCYP1A1/1A2, Cyp1a KO, WT and HRN mice

Data are mean ± SD (% mean of C57BL/6J ± %SD); n=4; * -Significantly different from C57BL/6J (unpaired t test; two tailed p values; * - p<0.05; ** - p<0.01; *** - p<0.001; **** - p<0.0001)

Mouse line	**C_{max}** ng/ml	**V/F(obs)** ml/kg	**HL** h	**AUCinf(obs)** h*ng/ml	**CL/F(obs)** ml/h/kg
C57BL/6J	2383±628 **(100±26)**	1253±494 **(100±39)**	0.94±0.25 **(100±27)**	5704±1265 **(100±22)**	905±170 **(100±19)**
Cyp1a KO	3991±472** **(167±20)**	992±188 **(79±15)**	2.39±0.2*** **(253±22)**	17651±2073**** **(309±36)**	286±35*** **(32±4)**
hCYP1A1/1A2	3082±194 **(129±8)**	1111±55 **(89±4)**	1.3±0.33 **(138±35)**	8397±1797* **(147±32)**	615±121* **(68±13)**
HRN	3744±794* **(157±33)**	1057±82 **(84±7)**	8.4±0.8**** **(891±85)**	57271±2583**** **(1004±45)**	87±3.8**** **(9.7±0.42)**

C_{max} is maximum observed concentration; HL is terminal half-life; AUCinf(obs) is area under the curve from dosing time extrapolated to infinity from the last observed caffeine concentration; V/F(obs) is volume of distribution calculated using AUCinf(obs) and CL/F(obs) is clearance calculated using AUCinf(obs)

Table 3: Contribution of CYP1A2 to caffeine systemic clearance calculated from published mouse studies

The difference between caffeine systemic clearance in the defined mouse strain and that in the Cyp1a KO mouse line was divided by the value of the systemic clearance in the defined mouse strain and then multiplied by 100% to obtain contribution of CYP1A2. Clearance value measured in CYP1A2$^{-/-}$ mice was used to calculate CYP1A2 contribution to caffeine systemic clearance in C57BL/6N mice reported by Buters et al (Buters et al., 1996).

Mouse line	Dose mg/kg	Route	Clearance ml/(h*kg)	Reference	CYP1A2 contribution %
CYP1A2$^{-/-}$	2	IP	276	(Buters et al., 1996)	0
C57BL/6N	2	IP	2268	(Buters et al., 1996)	88
Cyp1a KO	5	PO	286	This study	0
C57BL/6J	5	PO	905	This study	68
hCYP1A1/1A2	5	PO	614	This study	53
C57BL/6J	5	PO	472*	(Li et al., 2017)	39
Swiss	20	PO	311†	(Samojlik et al., 2016)	8
Swiss	20	IP	398†	(Samojlik et al., 2016)	28
C57BL/6J	5	PO	726	(Scheer et al., 2014)	61
CD-COBS	1	IV	732	(Walton et al., 2001)	61
CD-1	20	IP	640	(Kaplan et al., 1990)	55
CD-1	40	IP	380	(Kaplan et al., 1990)	25

PO = per os (oral gavage); IP = intraperitoneal: IV - intravenous

* - as it was not clear if the AUC reported in the paper was an AUCinf, caffeine clearance was calculated from C57BL/6J mean pharmacokinetic profile presented on Fig. 2 in the publication (Li et al., 2017); † - clearance was calculated by dividing dose by AUCinf;

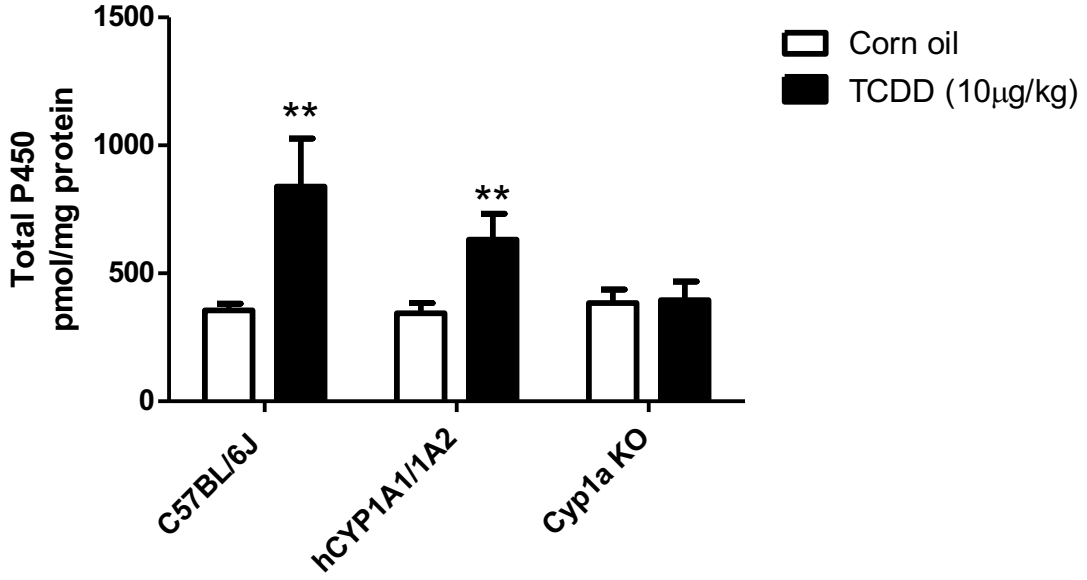

Figure 1

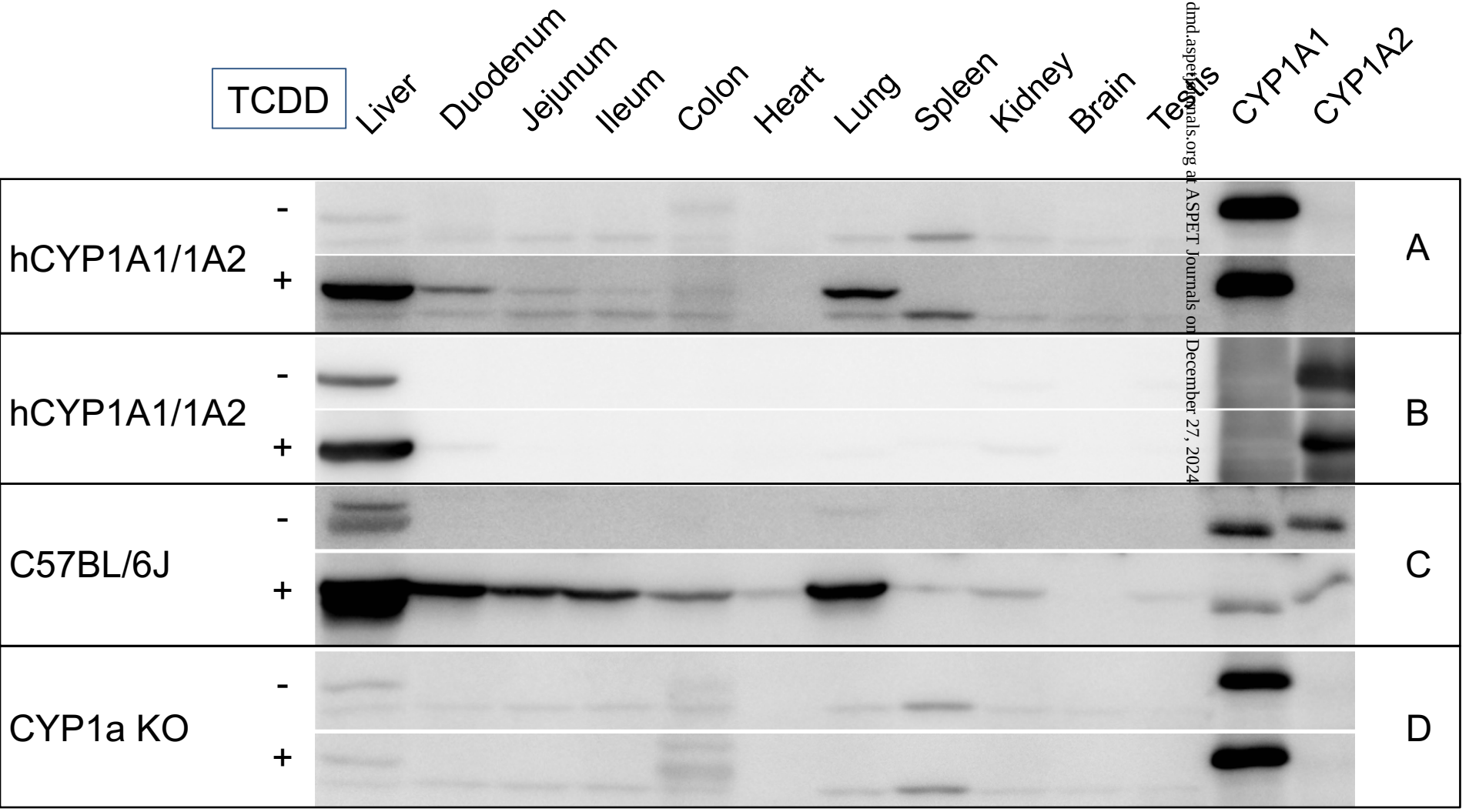

Figure 2

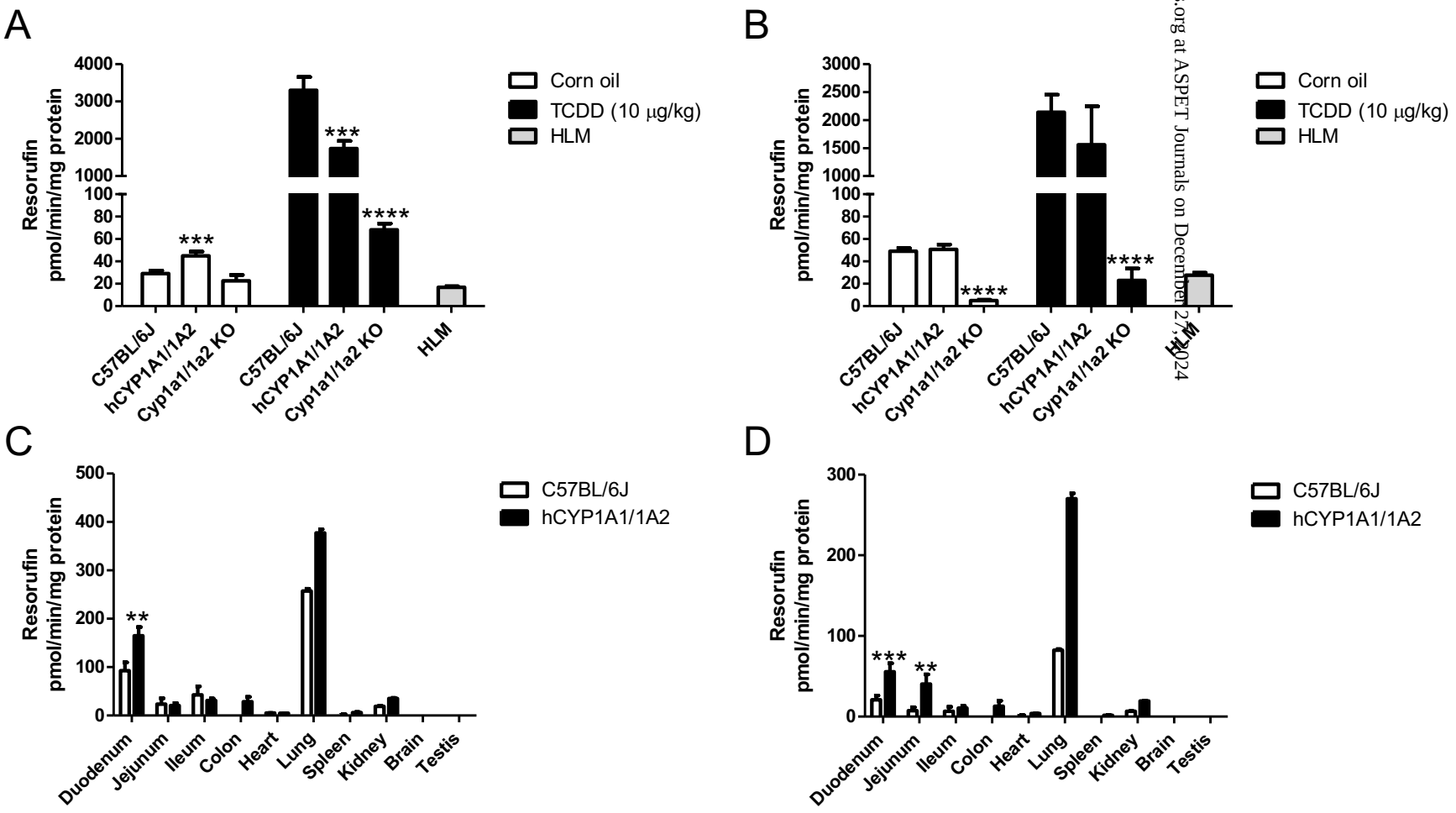

Figure 3

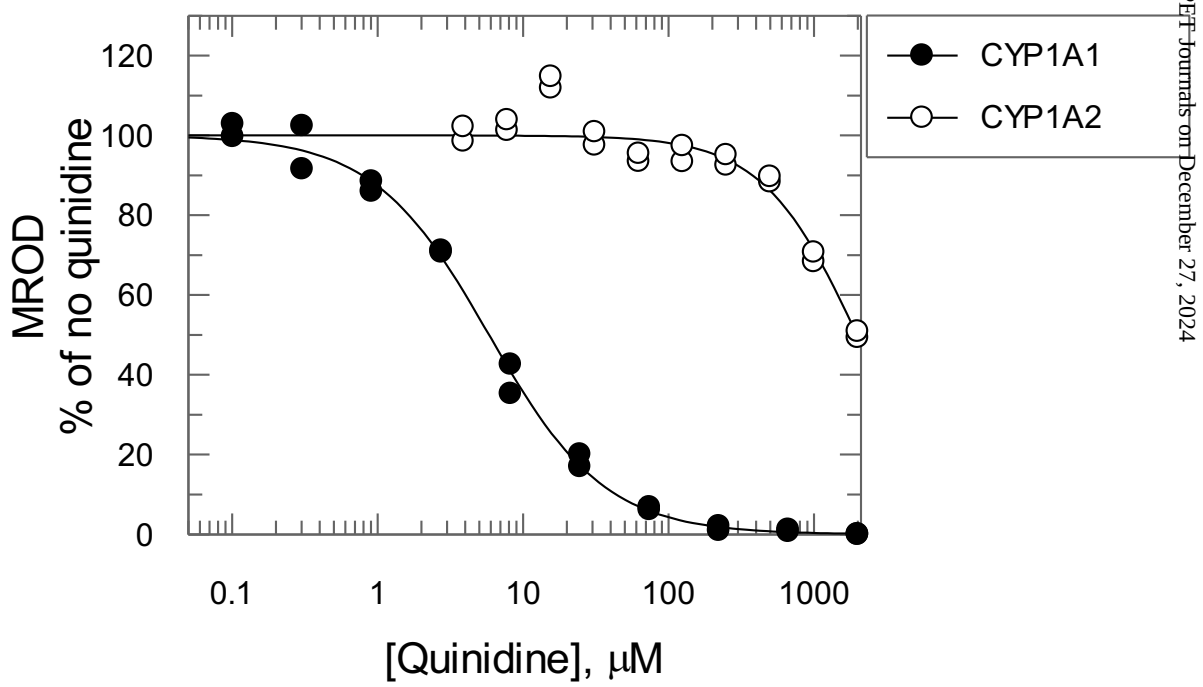

Figure 4

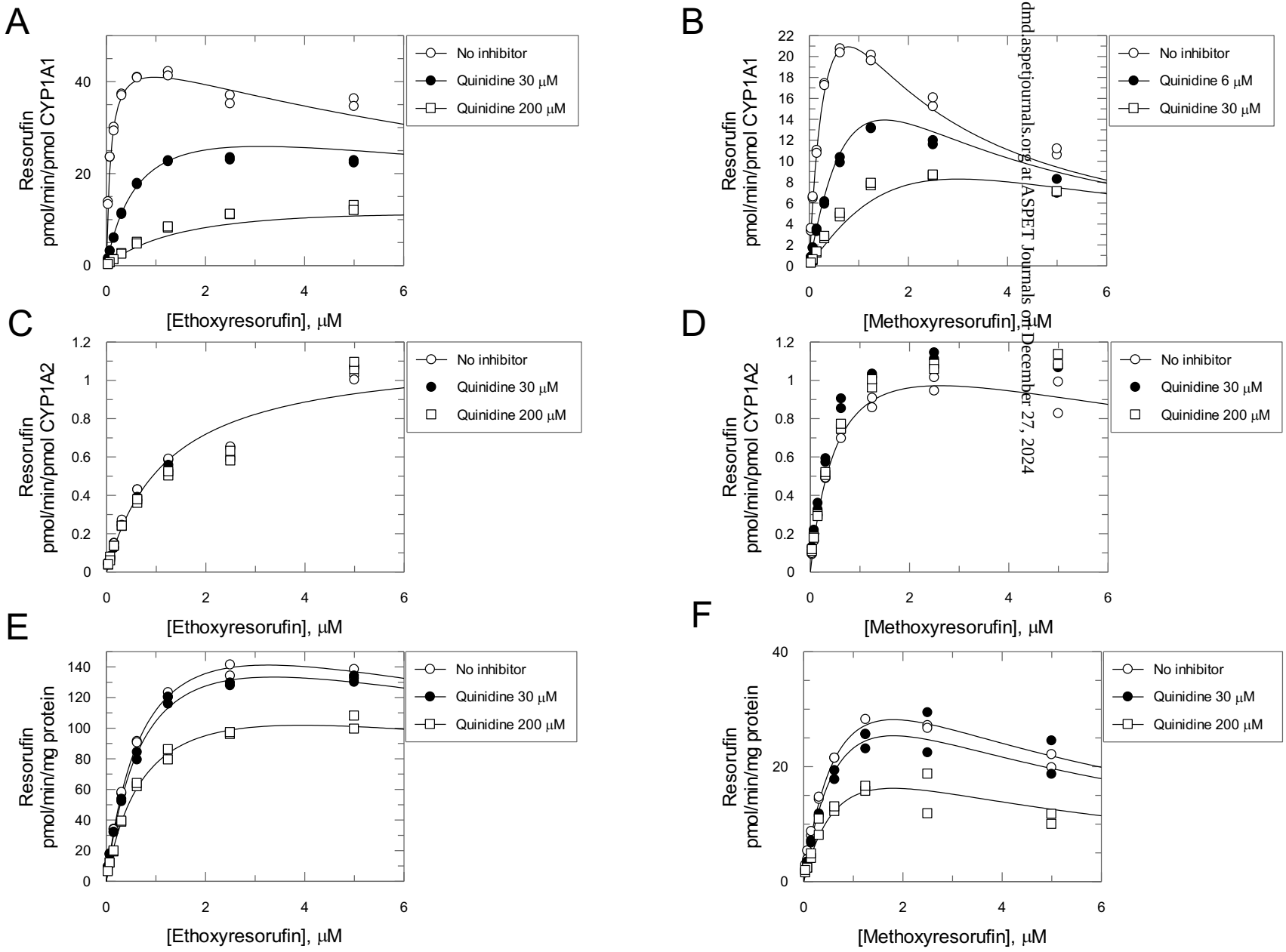

Figure 5

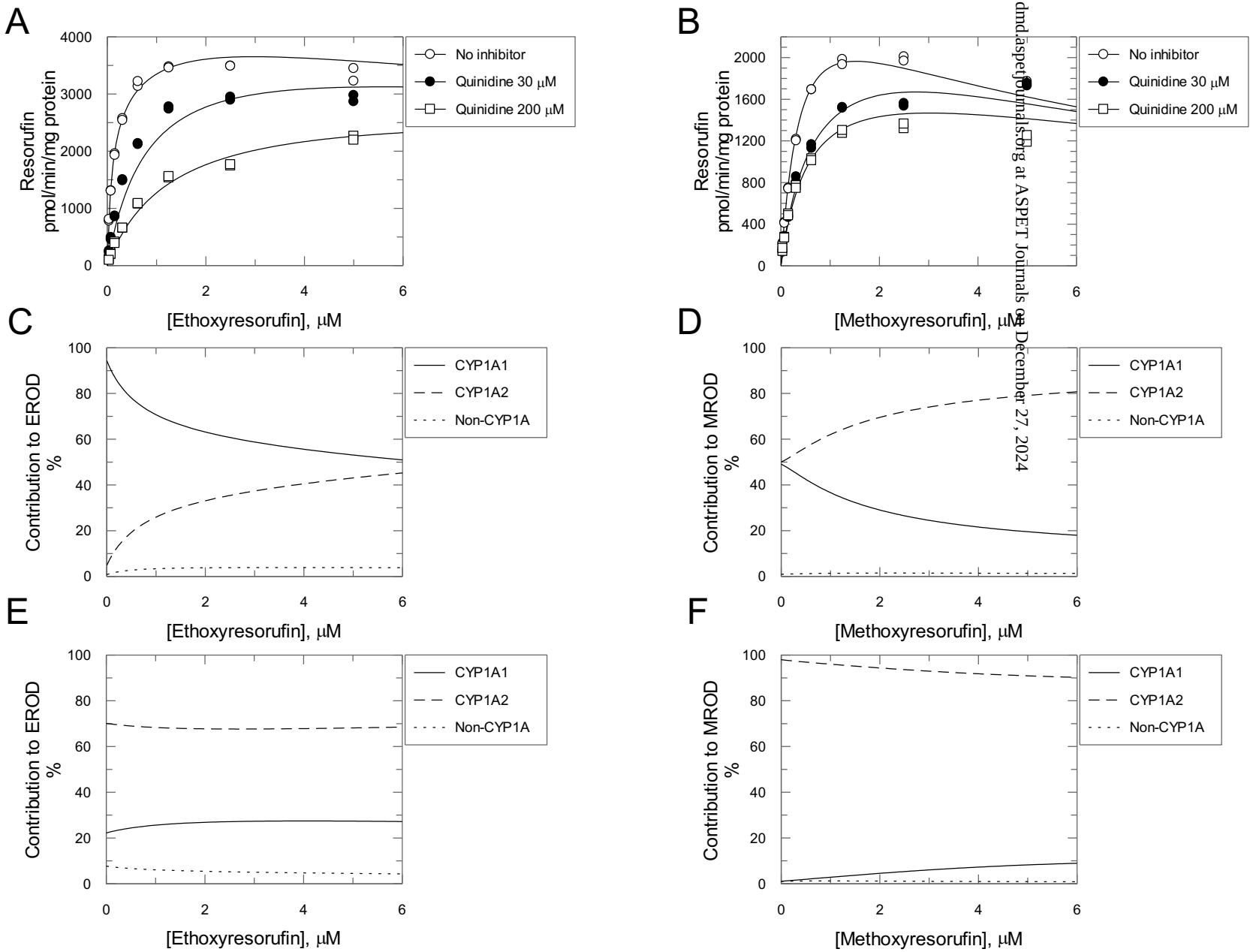

Figure 6

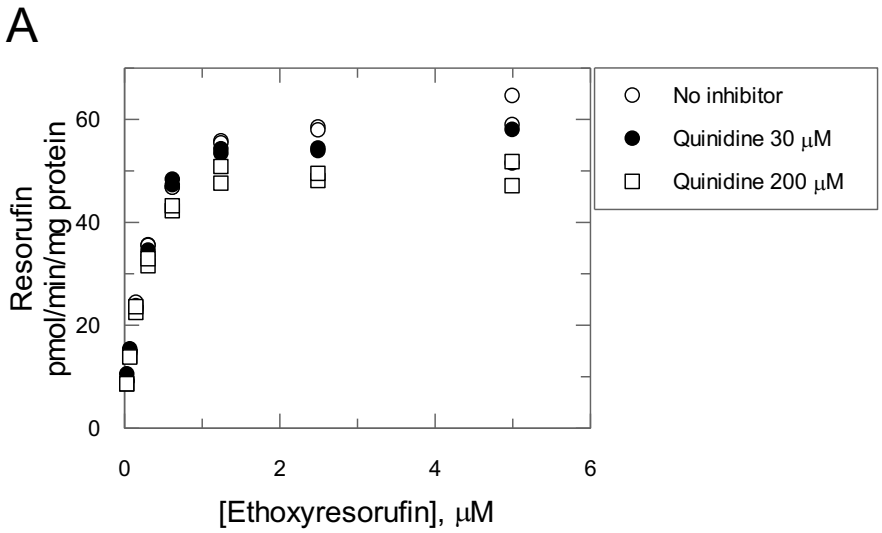

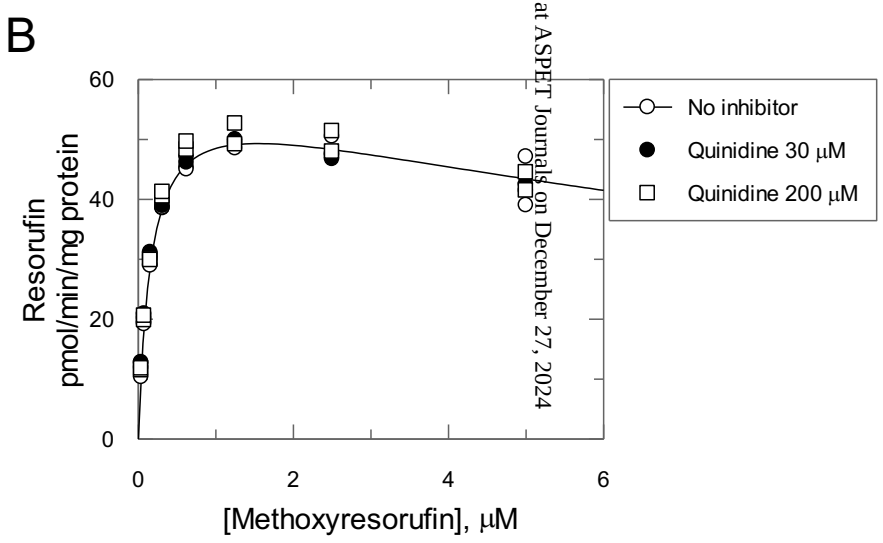

Figure 7

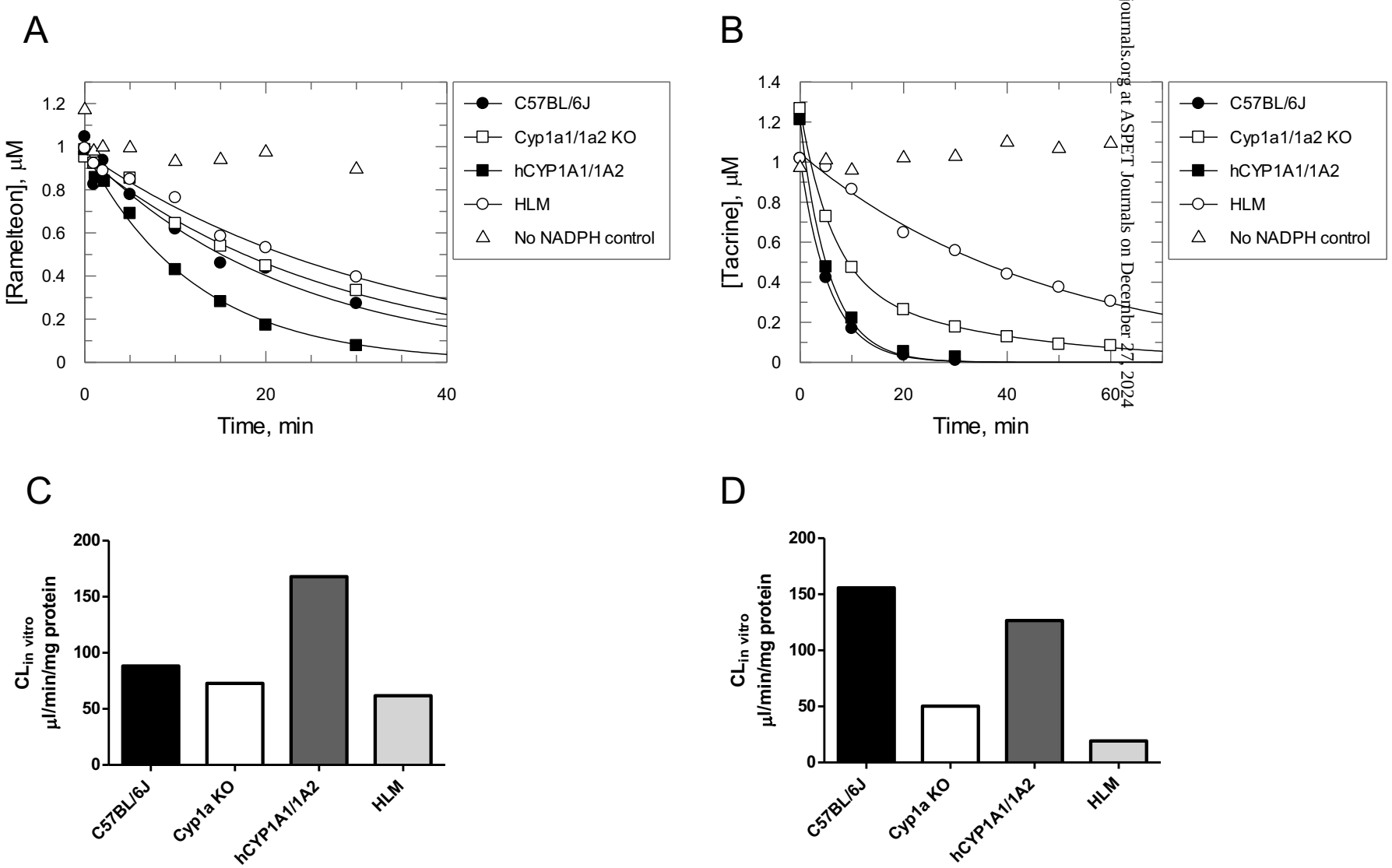

Figure 8

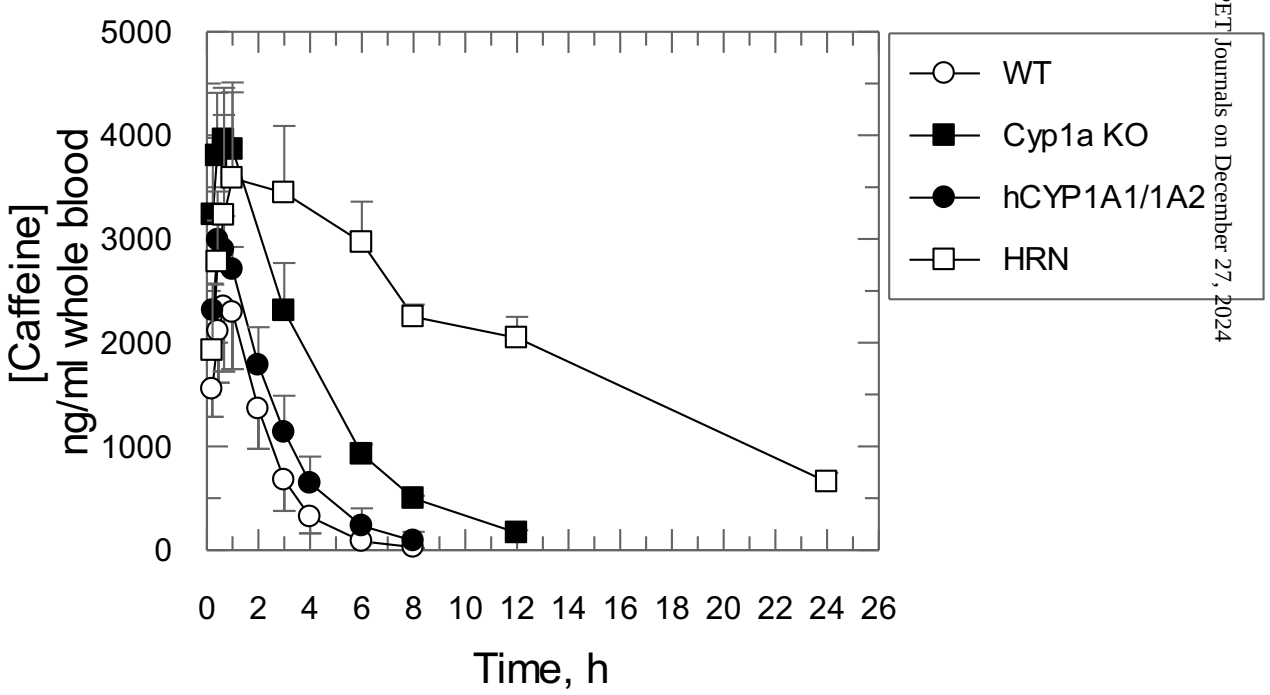

Figure 9

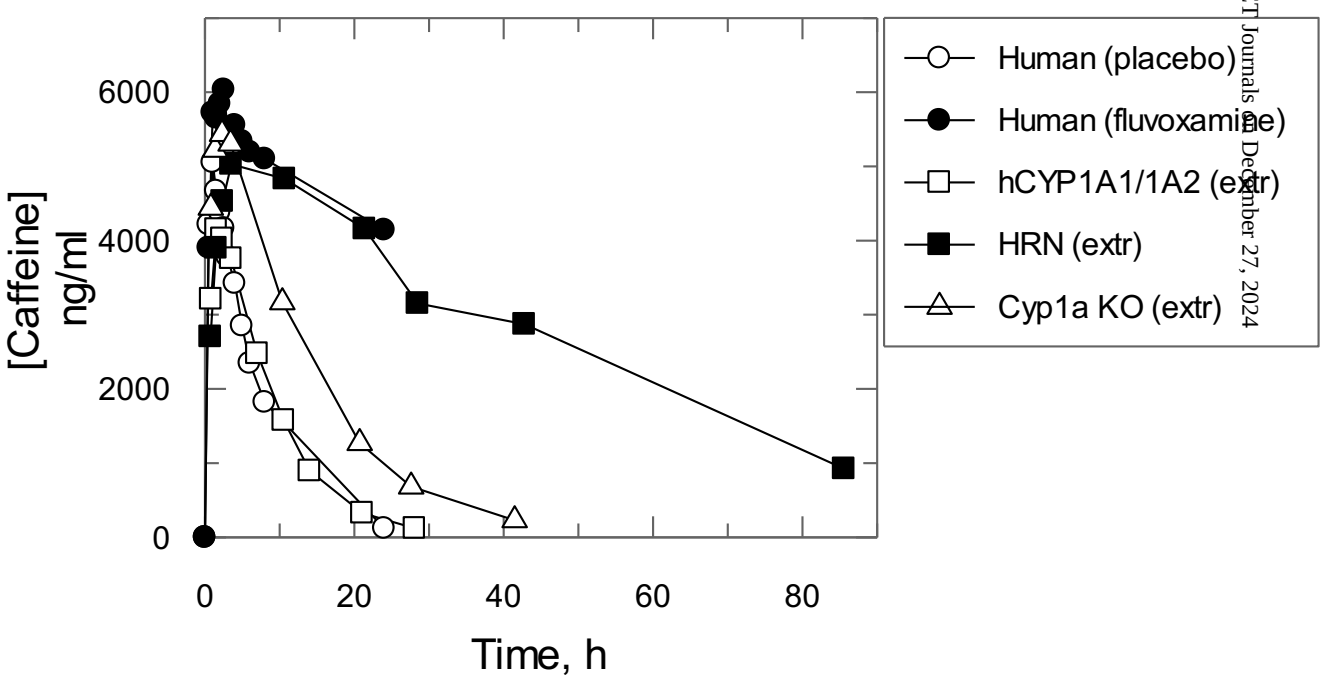

Figure 10

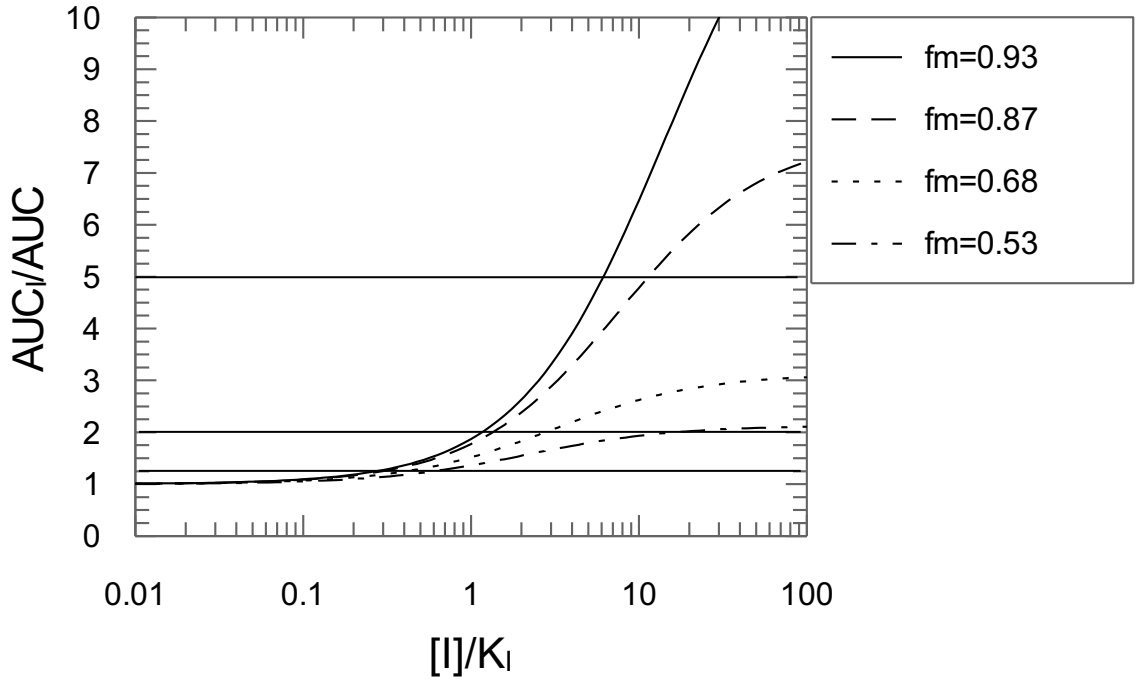

Figure 11